J. Fluid Mech. (1988), *vol.* 187, *pp.* 1-33
Printed in Great Britain

An investigation of the growth of turbulence in a uniform-mean-shear flow

By J. J. ROHR,† E. C. ITSWEIRE,‡ K. N. HELLAND‖ AND C. W. VAN ATTA¶

Institute for Pure and Applied Physical Sciences and Department of Applied Mechanics and Engineering Sciences, University of California, San Diego, La Jolla, CA 92093, USA

(Received 17 July 1986 and in revised form 20 April 1987)

A uniform-mean-gradient shear flow was produced using a ten-layer closed-loop water channel, providing long enough dimensionless flow development times ($\tau = (x/\bar{U})(\partial\bar{U}/\partial z)$) for the turbulence to grow. The rate of growth of the turbulence compares well with similar measurements in wind-tunnel-generated uniform shear flows for which the mean shears and centreline velocities are larger by an order of magnitude. Preliminary investigations were undertaken to study the growth of the turbulent intensity as functions of the mean shear, centreline velocity, and initial disturbance lengthscales. Initial disturbance lengthscales were varied by using grids of different mesh sizes.

Turbulent intensities were found to increase nearly linearly with τ. Differences in grid mesh size produce different offsets in the turbulent intensity level, with a larger grid mesh producing a higher positive offset. This offset persists throughout the growth of the turbulent intensity. These observations provide valuable insight in interpreting previous wind-tunnel measurements, in particular the high-shear experiments of Karnik & Tavoularis (1983). Comparison with the theoretical predictions of Tavoularis (1985) allows for an improved universal characterization of evolving turbulence in a uniform mean shear.

1. Introduction

One of the most fundamental properties of turbulent flows is the coupling of the turbulence to the mean shear of the flow through the mechanism of turbulent energy production. The simplest flow in which to study interactions between the turbulence and the mean flow is homogeneous turbulence sustained by a constant mean shear, as first conceived by von Kármán (1937). Corrsin (1963) later suggested how this flow could be set up in the laboratory. Laboratory homogeneous shear flow was initially understood to be an idealization only in the sense that homogeneity strictly requires an infinite spatial field. However, more fundamentally, the experiments of Champagne, Harris & Corrsin (1970, hereinafter referred to as CHC) showed that even when the turbulent intensities and stresses are both effectively homogeneous, the turbulent integral lengthscale grows downstream. Subsequently, Harris, Graham & Corrsin (1977, hereinafter referred to as HGC) found that given sufficient flow development time, the turbulence intensities also increase monotonically down-

† Present address: NOSC, Code 634 San Diego, CA 92152, USA.
‡ Present address: Chesapeake Bay Institute, Johns Hopkins University, Baltimore, MD 21211, USA.
‖ Also: Data Ready, Suite 150 4647T Highway 280, East Birmingham, AL 35243, USA.
¶ Also: Scripps Institution of Oceanography.

stream. Experimental evidence for the lack of vertical homogeneity was obtained by HGC and Tavoularis & Corrsin (1981, hereinafter referred to as TC) when they observed the Taylor microscale to increase in the direction of increasing mean velocity.

The fact that a perfectly homogeneous shear flow is in principle not realizable does not diminish the motivation for study laboratory flows which approximate ideal conditions. As pointed out by CHC, if one could avoid the complicating effects imposed by the proximity of the boundaries, a more natural relation between the turbulence and the mean velocity gradient could be studied. For most turbulent shear flows the size of the large eddies responsible for the bulk of the turbulent shear stress is of the same order as the scale of the mean-flow variation. For the laboratory studies of uniform-gradient shear flow, however, the lengthscales of the turbulence can be made small compared with the lengthscale over which the mean velocity gradient is constant (imposed by the facility size). These scales are thus able to evolve more freely while interacting with an essentially uniform mean shear, thereby providing a test case for the verification of general turbulence theories and direct numerical simulations.

Although much was learned from previous experiments on 'nearly' homogeneous unstratified shear flow, they did not produce a satisfactory quantitative understanding of the downstream turbulent growth. Rose (1966), CHC and Mulhearn & Luxton (1975) found that the turbulent component kinetic energies and shear stress reach constant values while both the integral and Taylor lengthscales exhibit continuing growth. However, when HGC extended CHC's measurements to larger dimensionless downstream times $\tau = (x/\bar{U})(\partial\bar{U}/\partial z)$, they found that the turbulence appeared to reach an asymptotic state in which the turbulence intensities and integral scales grew monotonically while the Taylor microscale remained constant. They also offered theoretical arguments predicting an asymptotically linear increase of turbulent kinetic energy and found a plausible degree of linearity in their downstream growths. When TC measured the velocity in the same flow field with more reliable digital techniques, they found that the downstream growth of the three components of the turbulent kinetic energy was well represented by parabolic growth. Later, Tavoularis (1985) found that the same data could be fitted by a weak exponential growth in agreement with his semi-analytical prediction. The most recent wind-tunnel measurements by Karnik & Tavoularis (1983, hereinafter referred to as KT) for larger dimensionless development times τ corroborate this exponential growth rate. It is evident that further work is required to reconcile the different experimental results found for the growth of turbulence in a uniform mean shear.

None of these earlier experiments were able to establish how the growth rate of the turbulence depends on the mean velocity gradient for a given mean centreline velocity. HGC and TC's measurements were taken for the same mean shear and centreline velocity in the same wind tunnel. Although KT were able to produce different values of the mean shear, it was at the expense of severely changing the centreline velocity. In all these wind-tunnel experiments the initial velocity of each layer was produced by a single commmon air supply. The shear was created by placing non-uniform resistances in each layer of the flow. This technique makes it very difficult to control the flow because the adjustment of the resistance in any one layer changes the input to the other layers. In our facility each layer has its own separate pump and feeding system, so that we could, for the first time, begin to

isolate the effect of changing the mean shear while keeping the other parameters of the flow nearly constant.

Another important phenomenon not sufficiently explored is whether or not different initial-lengthscale disturbances have any effect on the far-field-growing turbulence. Rose (1970) generated several different initial lengthscales by placing grids of different mesh sizes at the beginning of his test section, while keeping the mean shear nearly constant. Unfortunately, his measurements did not extend far enough in dimensionless time τ to observe any growth of turbulence. This led Rose (1970) to the erroneous conclusion that the grid-imposed lengthscale determines a constant energy level for the turbulence. Although KT had both large τ-values and different grid mesh sizes they could not reproduce the same mean velocity field when the grid was changed. KT also did not interchange grids at the same position in their flow. The present facility allowed us to maintain nearly the same shear when the size of the initial disturbance lengthscale was changed and to have development times large enough to ensure turbulent growth. We were thus able to isolate the influence of the initial disturbance lengthscale on the downstream growth of the turbulence.

2. Experimental facility and instrumentation

2.1. *Facility improvements*

The water channel used in the present experiments was designed for the study of stably stratified turbulent flows with uniform or sheared mean velocity profiles. The basic facility has been described in detail by Stillinger *et al.* (1983) and a general sketch of it is shown in figure 1 (*a*). Some important modifications were made to the original turbulence management section to improve the initial homogeneity of the mean flow and increase the mean shear. The new turbulence management section is shown in figure 1 (*b*). Here as in all the figures the downstream, vertical and cross-stream directions are designated as x, z and y respectively. All ten layers are identical, nine of which are shown in figure 1 (*b*) with only the top layer drawn in full detail. The previous Stillinger *et al.* (1983) turbulence management section for a constant mean shear consisted of a screen (6 mm mesh) backed by 2.5 cm thick acoustic foam placed directly against the inlet splitter plates. No other screen–foam combination was used downstream to avoid destroying the velocity shear and the density gradient (when used). Detailed laser-Doppler-velocimeter measurements of the mean velocity field for sheared flows showed large-scale inhomogeneities in the form of jet-like structures near the sidewalls of the test section. In addition, the design of the outlet of the test section, which requires the use of individual sluice gates to match the flow rate layer by layer, causes enough pressure drop to raise the height of water in the test section from 25.4 cm to 30 cm for the largest shear. This abrupt jump in water level, which occurred at the end of the management section, was found to be responsible for high velocity fluctuations and a rapid downstream degradation of the mean shear. Such effects were found unacceptable and prompted a number of improvements.

A smooth ten-layer diffuser 60 cm long was built of stainless-steel sheets 1.6 mm thick to expand the height of each layer from 2.54 to 3.05 cm. The entrance to the diffuser was adjusted to match the inlet splitter plates so that each layer was isolated from the adjacent layers. Upstream of the diffuser each inlet layer was filled with a 5 cm long coated aluminium honeycomb (6 mm hexagonal mesh) to break up the large-scale structures of the incoming flow. Each layer of the diffuser section had two

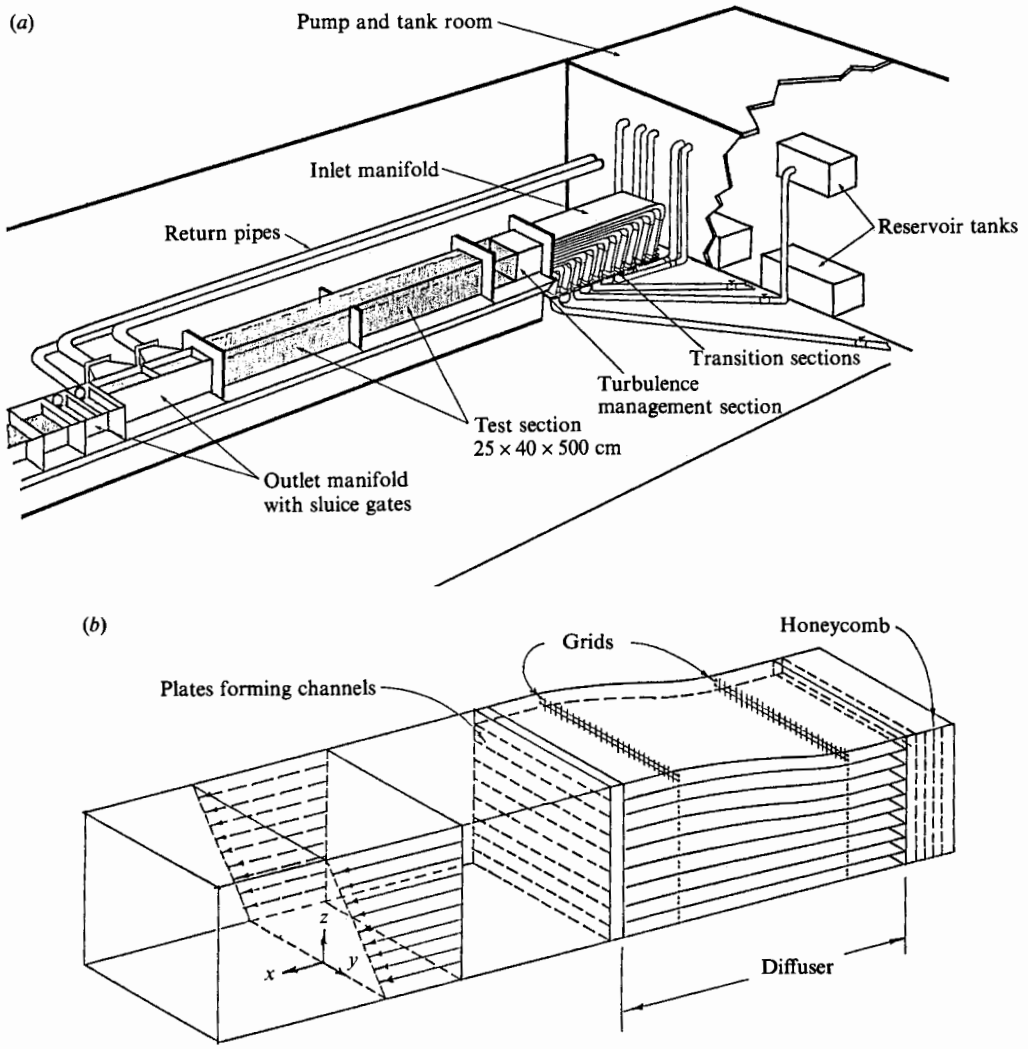

FIGURE 1. (a) Perspective sketch of water-tunnel system. (b) Perspective sketch of inlet (turbulent management) section.

biplane grids (9 mm mesh) made of stainless-steel welding rods with diameter 1 mm located 5 and 50 cm downstream of the honeycomb. Several combinations of grids and screens with various mesh sizes and solidities were tested and the present configuration worked best in reducing mean-flow distortion and background turbulence.

2.2. *Downstream velocity development*

Figure 2(a) shows the cross-stream (y-direction) variation of the mean velocity profiles at $x/M = 15$ downstream from a biplane grid with mesh size $M = 1.52$ cm for various heights z. ($x/M = 15$ is equivalent to $x/H = 1.3$, where $H = 30.5$ cm is the depth of the water in the channel.) The biplane grid, which provided mixing to smooth the initially step-shaped velocity profile, was located 3 cm from the end of the diffuser and was designed to match the 3.05 cm high layers of the diffuser. The five heights for the measurements of figure 2(a) were taken at the middle of layers

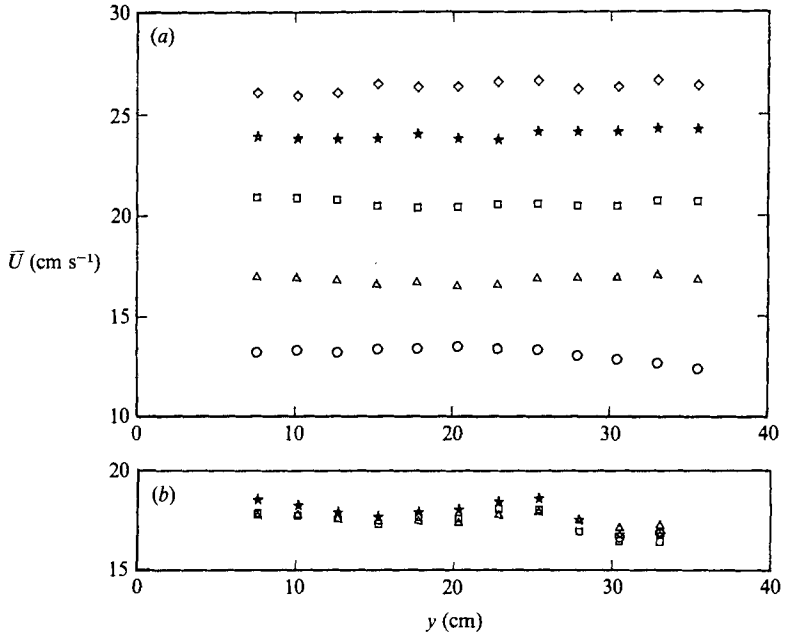

FIGURE 2. (*a*) Representative horizontal velocity profiles at $x/H = 1.3$; ○, $z = 10.7$ cm; △, 13.7 cm; □, 16.8 cm; ★, 19.8 cm; ◇, 22.9 cm. (*b*) Representative downstream evolution of the horizontal velocity profile at $z = 14$ cm; △, $x/H = 2.8$; □, 4.7; ★, 6.6. Channel width is 40 cm, depth of water (H) is 30.5 cm.

4–8. Typically, the measurements reported were taken at a height of 15 cm from the bottom and at $y = 20$ cm (the centreline of the test section). Here, far from the boundary layers of the sidewalls, the cross-stream variation of the mean velocity was small and, as seen in figure 2(*b*), remained so further downstream. Figure 3(*a*) shows an example of a typical mean vertical velocity profile for the shear experiments with an upstream grid of mesh size $M = 1.52$ cm, and solidity $\sigma = 31\,\%$. The degradation of the velocity profile in figure 3(*a*) is greater than that found in comparable wind-tunnel studies where, unlike the UCSD water channel, the walls could be adjusted to compensate for boundary-layer growth. In wind-tunnel experiments where no adjustment was made to compensate for boundary-layer growth (see Webster 1964), the initial linear velocity profile also decayed appreciably downstream. The amount of change of the mean velocity field necessary to balance the growth of the turbulence is very small. If, for example, we attribute all the downstream growth of $\overline{u^2}$ to the mean transport term $\bar{U}(\partial\bar{U}/\partial x)$, the change in the local mean velocity would only be about 1%. As seen in figure 3(*a*) the central part of the vertical velocity gradient changes slowest and remains nearly linear. All measurements reported here are restricted to this region which remains larger than the evolving turbulent integral scale (l).

The background root-mean-square velocity fluctuations measured at the inlet (without the grid) were less than 2% of the local mean velocity. No horizontal cross-stream (y) velocity fluctuation measurements were made. Vertical fluctuation measurements at the inlet were found to be not as homogeneous as some of the previous wind-tunnel experiments (e.g. CHC, HGC, and TC). Moreover, as can be seen in figure 3(*b*), a systematic trend away from homogeneity was often found in the present water-channel experiments. Turbulent fluctuations in the slower layers were

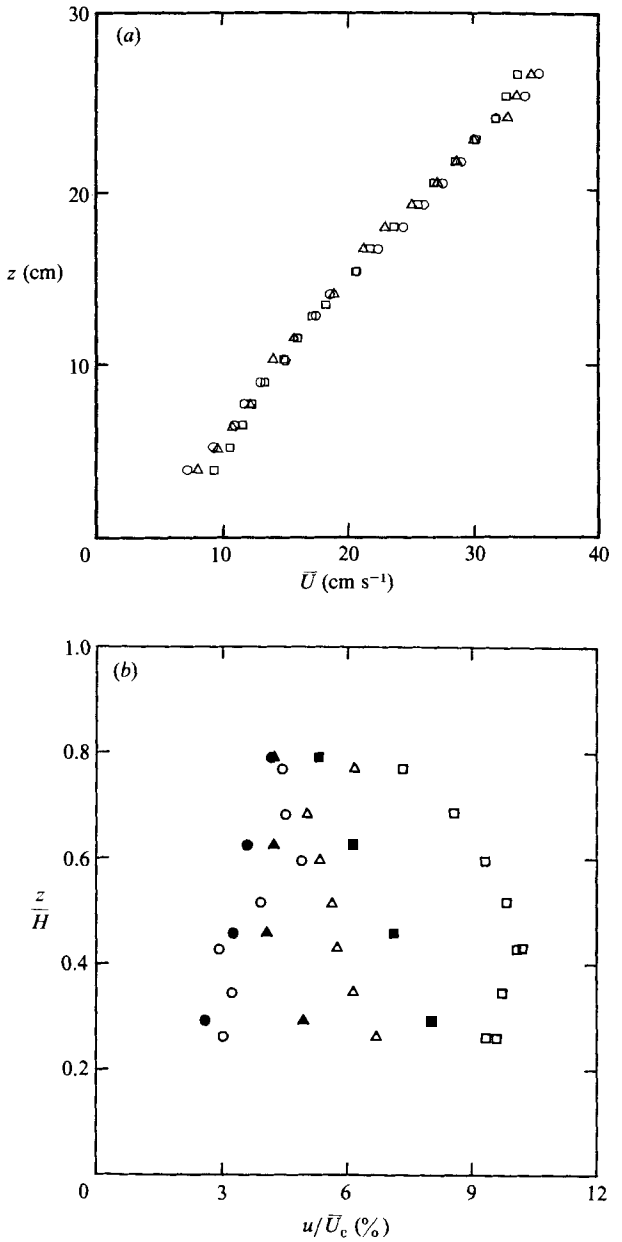

FIGURE 3. (*a*) Representative downstream evolution of the vertical velocity profile along the centreline ($y = 20$ cm) of the test section; ○, $x/H = 2.2$; △, 5.3; □, 10.3. (*b*) Representative downstream evolution of the vertical profile of the longitudinal turbulent intensities. Solid symbols denote present water-channel measurements: ●, $x/H = 2.2$; ▲, 5.3; ■, 11.6; $H = 30.5$ cm. Open symbols from KT: ○, $x/H = 1.04$; △, 7.5; □, 13; $H = 30.5$ cm.

observed growing downstream at a faster rate. Although no mention of this unequal growth of turbulent fluctuations along the mean shear has appeared in the past literature (perhaps larger flow development times and the water channel's accelerated decay of the mean shear exaggerates this aspect of the flow) there are arguments presented herein (§6) which suggest such a possibility. Also included in figure 3(*b*) are

wind-tunnel measurements of KT which extend to large τ-values and also exhibit along the mean shear increasing downstream inhomogeneity. Regardless of these differences, the downstream evolution of turbulent intensities and lengthscales observed in the water channel are in excellent agreement with previous wind-tunnel observations.

2.3. *Instrumentation*

Quartz-coated TSI X-films provided measurements of the downstream and vertical velocity components, while a Platinum Resistance Thermometer (PRT) measured the mean temperature variations required to compensate for overheat changes of the films. The hot films were standard TSI quartz-coated cylindrical sensors for use in water with a 50 μm diameter and a 1 mm sensing length. The mean temperature increase due to pump losses and viscous dissipation was about 1 °C/h and hot-film overheats varied from 13 to 10 °C from the beginning to the end of an experiment. Even at low overheats dissolved gases in the water come out of solution forming bubbles on the hot films. This changes the heat transfer characteristics of the film, imparting a low-frequency drift to the data. Bubbles were swept away by periodically injecting a high-pressure stream of air from a nozzle below and behind the X-film, allowing about 15 s of uncontaminated data. Ten seconds of data were normally taken so that frequencies down to 0.1 Hz would be resolved.

The X-film sensor was calibrated by towing the motor-driven instrumentation cart at a monotonically increasing speed through the still water of the test section. The towing speeds that were obtained from the variable-speed d.c. motor ranged from 10 to 40 cm/s. The velocity of the cart was measured by differentiating its position with respect to time. Several tows were made before and after an experiment at yaw angles of 0° and $\pm 10°$, a range adequate for the low-intensity turbulence produced. Enough time was allowed between tows for the water in the test section to come to rest. The modified King's law proposed by Castaldini, Helland & Malvestuto (1980) satisfactorily described the heat transfer law of the hot films:

$$\frac{E_b^2}{T_f - T} = A + B\left(\frac{U}{\rho}\right)^n, \tag{1}$$

where E_b is the bridge voltage, U, ρ and T are respectively the velocity, density and ambient temperature of the water, and T_f the film temperature. The exponent n varied between 0.25 and 0.30 for different films. Following the error analysis of Stillinger (1983), temperature contamination of the velocity components was found to be negligible. From (1) linearized voltages were computed as

$$E_1 = \left(\frac{E_b^2/(T_f - T) - A}{B}\right)^{\frac{1}{n}}. \tag{2}$$

Assuming a cosine law appropriate for low-intensity turbulence, a first-order two-dimensional least-squares fit was performed in terms of the linearized voltages.

3. Analytical and theoretical framework

The corresponding theoretical problem is to determine the statistical state of an evolving uniform mean-shear flow, which is governed by the continuity and Navier–Stokes equations. Since the full Navier–Stokes equations are not presently mathematically tractable, the problem becomes one of acquiring correct insight from them without explicitly solving them. Therefore, some initial assumptions must be

judiciously chosen and experimentally appraised before any attempt is made at a semi-analytical solution. For wakes, jets, and mixing layers, the region of turbulent flow is extremely elongated in the main flow direction, and it is reasonable to simplify these equations by applying the boundary-layer approximations. No such approximations are appropriate for the case of a uniform mean shear, as the turbulence is now distributed both vertically and horizontally throughout space. In the past, different degrees of homogeneity have been assumed to simplify the equations.

CHC began with the simplest possible assumption of rectilinear mean flow, i.e. $\bar{U} = \bar{U}(z,t)$, $\bar{W} = \bar{V} = 0$, and the restriction to homogeneity for all averages except $\bar{U}$. With these assumptions CHC could then deduce greatly simplified equations for the mean flow and turbulent kinetic energy. Mean and fluctuating velocities in the downstream (x), vertical (z) and cross-stream (y) directions are represented, respectively, as $\bar{U}$, u, $\bar{W}$, w, and $\bar{V}$, v. Mean and fluctuating pressures are similarly represented as $\bar{P}$, p. The simplified equations are

$$\frac{\partial \bar{U}}{\partial x} = 0 \quad \text{mean-continuity equation,} \tag{3}$$

$$\frac{\partial \bar{U}}{\partial t} = 0 \quad \text{mean-momentum equation,} \tag{4}$$

$$\frac{\partial}{\partial t}(\tfrac{1}{2}\bar{U}_j\bar{U}_j) = \overline{uw}\frac{\partial \bar{U}}{\partial z} - \frac{\partial}{\partial z}(\bar{U}\,\overline{uw})$$

$$+\nu\frac{\partial^2}{\partial z^2}(\tfrac{1}{2}\bar{U}_j\bar{U}_j) - \nu\left(\frac{\partial \bar{U}}{\partial z}\right)^2 = 0 \quad \text{mean-kinetic-energy equation,} \tag{5a}$$

$$\frac{\partial}{\partial t}(\tfrac{1}{2}\overline{q^2}) = -\overline{uw}\frac{\partial \bar{U}}{\partial x} - \nu\overline{\frac{\partial u_i}{\partial x_k}\frac{\partial u_i}{\partial x_k}} \quad \text{turbulent-kinetic-energy equation,} \tag{5b}$$

where $q^2 = u^2 + w^2 + v^2$ and Einstein's summation convention has been employed. For an incompressible Newtonian fluid, the total mean stress tensor expressed in indicial notation is

$$T_{ij} = -\bar{P}\delta_{ij} + \mu\left(\frac{\partial \bar{U}_i}{\partial x_j} + \frac{\partial \bar{U}_j}{\partial x_i}\right) - \rho\overline{u_i u_j}, \tag{6}$$

so that for steady flow the mean-kinetic-energy equation with CHC's assumptions can be expressed as

$$0 = \frac{\partial}{\partial z}(T_{xz}\bar{U}) - T_{xz}\frac{\partial U}{\partial z}. \tag{7}$$

This is also the form of the mean-kinetic-energy equation for fully developed turbulent Couette flow (Tennekes & Lumley 1972). As seen from (7) a constant stress field does not change the flow's mean kinetic energy because the first term on the right-hand side of (7), representing the transport of mean-flow energy by the stress, is exactly balanced by the deformation work $T_{xz}(\partial\bar{U}/\partial z)$. It is expected that the deformation work will decrease the energy of the mean flow unless this loss is balanced by an external input of energy. In Couette flow this external energy input is provided by the moving boundaries, but there is no such source of energy in the present case. On the contrary, as Hinze (1975) points out, the continuous generation of turbulence by the mean shear flow must decrease the mean velocity gradient, and in the process of satsifying continuity generates a compensating $\bar{W}$-flow along the direction of the mean shear. The fact that theoretically the mean velocity gradient

cannot remain constant does not mean necessarily that it is an inappropriate approximation.

When HGC extended the range of τ and observed downstream growth of the turbulent fluctuations, CHC's previous homogeneous assumptions had to be relaxed. The assumptions of HGC became

(i) steady rectilinear mean flow,
(ii) $\bar{W} = \bar{V} = 0$,
(iii) $\partial\bar{U}/\partial y = 0$,
(iv) $\partial\bar{U}/\partial z =$ constant,
(v) all turbulent moments are only transversely homogeneous

$$(i.e.\ \partial(\overline{\ })/\partial z) = \partial(\overline{\ })/\partial y = 0).$$

Equations (3)–(5) then become

$$\frac{\partial\bar{U}}{\partial x} = 0 \quad \text{mean-continuity equation,} \tag{8}$$

$$\frac{\partial\bar{P}}{\partial x} = -\rho\frac{\mathrm{d}(\overline{u^2})}{\mathrm{d}x}, \tag{9a}$$

$$\frac{\partial\bar{P}}{\partial z} = -\rho\frac{\mathrm{d}(\overline{uw})}{\mathrm{d}x} \quad \text{mean-momentum equations,} \tag{9b}$$

$$\frac{\partial\bar{P}}{\partial y} = 0, \tag{9c}$$

$$\bar{U}\frac{\partial(\frac{1}{2}\overline{q^2})}{\partial x} = -\overline{uw}\frac{\partial\bar{U}}{\partial z} - \frac{\partial}{\partial x}\overline{u(\tfrac{1}{2}q^2)} - \frac{1}{\rho}\frac{\partial}{\partial x}(\overline{up}) + \nu\frac{\partial^2}{\partial x^2}(\tfrac{1}{2}\overline{q^2}) - \epsilon \quad \text{turbulent-kinetic-energy equation,}$$

where $\epsilon = \nu\overline{\frac{\partial u_i}{\partial x_k}\left\{\frac{\partial u_i}{\partial x_k} + \frac{\partial u_k}{\partial x_i}\right\}}$ = mean-turbulent kinetic-energy dissipation.

HGC's assumptions (i–v) are shared by Tavoularis (1985), TC and KT. As shown by HGC, (9*a*, *b*) without any further approximations determine that $\partial(\overline{uw})/\partial x$ is a constant. This result, together with the compelling experimental evidence of HGC, TC and KT that $\overline{uw}/u'w'$ and $\overline{u^2}/\overline{w^2}$ (where $'$ indicates r.m.s. value) are constant downstream in their asymptotic range, constrains $\overline{u^2}$ and $\overline{w^2}$ to a linear growth with x. Although HGC had observed approximate linearity in the downstream growth of all three component energies, their data contain considerable scatter. When TC repeated these same measurements no linear growth was observed even though the data exhibited much less scatter. With the additional measurements of KT and the present results (§4) it is clear that the growth of turbulent kinetic energy is not linear but at least quadratic and perhaps weakly exponential.

Due to the discrepancy between the experimental results and HGC's theoretical predictions a closer examination of their initial assumptions is required. The assumption that $\bar{W} = \bar{V} = 0$ together with continuity requires that $\partial\bar{U}/\partial z = 0$, thus prohibiting energy transfer from the mean flow field. The observed downstream growth of $\overline{u^2}$ must then be balanced by a pressure gradient in the x-direction, as seen in (9*a*). This is in marked contrast with the free shear flows of jets, wakes, and mixing

layers where it is assumed that $\partial\bar{P}/\partial x = 0$. CHC, HGC and TC had all adjusted their wind-tunnel walls to acount for boundary-layer growth. CHC and TC report an essentially constant mean pressure over the test section within experimental accuracy. Unfortunately, the equivalent pressure gradient that could balance the measured term $-\rho(\partial\overline{u^2}/\partial x)$ (cf. (9*a*)) is too small to be determined accurately.

Another problem which follows from HGC's assumptions is that the resulting turbulent-kinetic-energy equation, (10), is inconsistent since the left-hand side depends linearly on z through $\bar{U}(z)$ while the right-hand side is allowed no z-dependence whatsoever. Experimentally, both HGC and TC find that the turbulent and viscous transport terms are negligible (typically less than 3% of the mean convective term). Therefore the approximate form of (10) is simply

$$\bar{U}\frac{\partial(\frac{1}{2}\overline{q^2})}{\partial z} \approx -\overline{uw}\frac{\partial\bar{U}}{\partial z} - \epsilon, \tag{11}$$

which still remains unbalanced in its z-dependence. Tavoularis (1985) achieves a balance without violating prior assumptions by letting the dissipation rate ϵ be a function of z as well as x. Both HGC and TC had observed that the Taylor microscale increases monotonically in the direction of increasing $\bar{U}(z)$ which implies that the dissipation rate decreases in the same direction. This leaves us in the awkward position of trying to imagine a pattern of motion which produces turbulence uniformly along the z-direction, but dissipates it at a slower rate along z with increasing $\bar{U}$. Tavoularis' assumptions, however, exclude such a possibility because the left-hand side of (11) can increase indefinitely with z while the maximum value of the right-hand side is bounded by $-\overline{uw}(\partial\bar{U}/\partial z)$, which is assumed to be constant along z.

The analysis of Tavoularis (1985), which predicts an exponential growth for the turbulent kinetic energy, is independent of the assumption that the dissipation but not the production term varies with distance along the mean shear direction (z). Starting with (11) and using the experimental evidence of CHC, HGC, TC and KT that ϵ/P (where $P = -\overline{uw}(\partial\bar{U}/\partial z)$), $\partial\bar{U}/\partial z$, and the dimensionless Reynolds stress $\overline{uw}/\overline{q^2}$ remain nearly constant with x in the asymptotic range, Tavoularis (1985) writes

$$\frac{\partial}{\partial x}(\overline{q^2}) - \left[\left(\frac{-\overline{uw}}{\overline{q^2}}\right)\frac{2}{\bar{U}}\left(1-\frac{\epsilon}{P}\right)\frac{\partial\bar{U}}{\partial z}\right]\overline{q^2} = 0, \tag{12}$$

where the coefficient of $\overline{q^2}$ is not a function of x. Equation (12) then has the simple exponential solution

$$\overline{q^2} = \overline{q_r^2}\exp\left[\left(\frac{-\overline{uw}}{\overline{q^2}}\right)\frac{2}{\bar{U}}\left(1-\frac{\epsilon}{P}\right)\frac{\partial\bar{U}}{\partial z}(x-x_r)\right] \tag{13}$$

where Tavoularis defines $\overline{q_r^2}$ as a reference value of the turbulent kinetic energy at a location $x = x_r$ within the asymptotic region. Note that (13) can be obtained without making any assumptions on the dependence of $\partial\bar{U}/\partial z$, $\overline{uw}$, $\overline{q^2}$, ϵ and P on z. The measurements of KT, for values of τ twice as large as those previously achieved, support Tavoularis' (1985) prediction for an exponential growth of the turbulent kinetic energy. This exponential growth must be weak, however, since TC's data are fitted equally well with parabolic (see TC, figure 5) or with exponential curves (see Tavoularis 1985, figure 1).

It can be shown that the necessary z-dependence of $\overline{uw}$ and possibly $\overline{\partial q^2}/\partial x$, needed to balance (11), can result from retaining the mean convective terms in the mean-

momentum equation. Assuming that the flow is steady, the viscous terms are negligible, and by symmetry $\bar{V}$ and $\partial(\overline{\ })/\partial y$ are both equal to zero, then the mean momentum equation for U reduces to

$$\bar{U}\frac{\partial \bar{U}}{\partial x}+\bar{W}\frac{\partial \bar{U}}{\partial z}+\frac{\partial \overline{u^2}}{\partial z}+\frac{\partial \overline{uw}}{\partial z}=-\frac{1}{\rho}\frac{\partial \bar{P}}{\partial x}. \tag{14}$$

Taking the derivative of this equation with respect to x, using continuity and assuming $\partial^2\bar{P}/\partial z\partial x$ is negligible, (14) reduces to

$$\bar{U}\frac{\partial}{\partial x}\left(\frac{\partial \bar{U}}{\partial z}\right)+\bar{W}\frac{\partial}{\partial z}\left(\frac{\partial \bar{U}}{\partial z}\right)=-\frac{\partial}{\partial z}\left(\frac{\partial \overline{u^2}}{\partial z}+\frac{\partial \overline{uw}}{\partial z}\right). \tag{15}$$

Therefore the degradation of the mean velocity gradient will cause inhomogeneity along z in terms which appear in (11) and could conceivably allow for a balance of the z-dependence in that equation.

In summary, we note that HGC and Tavoularis (1985) deduce quite different results while sharing identical assumptions. HGC deduced a linear growth of $\overline{q^2}$ with x from the mean-momentum equations while Tavoularis (1985) used the approximate turbulent-kinetic-energy equation (11) to deduce an exponential growth of $\overline{q^2}$ with x. Experiments have repeatedly shown (TC, KT) that the growth of $\overline{q^2}$ is not linear. This may imply that the unchanging-mean-flow-field assumption of HGC is inappropriate. Moreover by allowing the mean velocity gradient to decay (albeit slowly) a balance of the z-dependence in Tavoularis' (1985) approximate turbulent-kinetic-energy equation can be achieved. Establishing a firmer foundation for Tavoularis' theory is important since the predictions for this show best agreement with the experimental results.

4. UCSD water-tunnel results

Figure 4(*a*) shows the development of the longitudinal turbulent intensity ($u'/\bar{U}$) with x/H for different mean shears and mean centreline velocities but identical grid mesh, $M = 1.52$ cm. All measurements were taken on the centreline. H is equal to 30.5 cm, the depth of water in the channel, and x is the downstream distance measured from the grid. It is immediately apparent that when the mean centreline velocities are nearly the same (○, △), the turbulent intensities grow faster for the higher shear. Although this result may seem obvious, it is the first time that this effect has been demonstrated experimentally for the case of nearly constant centreline velocities. Also illustrated in figure 4(*a*) (○, □) is the effect of varying the centreline mean velocity while keeping the mean shear nearly constant. For the slightly higher-mean-shear data (□) the turbulence intensity is observed to increase spatially at a slower rate (in comparison to ○) presumably because the corresponding higher mean velocity allows less time for the turbulence to interact with the mean field. This is contrary to what was previously thought, as both KT and HGC expected that the mean velocity at the measurement location should not be a factor for determining the intensity and other statistics of the turbulence. Included in figure 4(*a*) are the corresponding wind-tunnel measurements of TC. TC had incorporated a rod along the centreline of the exit plane of each of their twelve channels. Since the thickness of the rod was comparable with the thickness of the channel separator plate, TC's equivalent mesh size (M) is approximated to be 1.5 cm.

The turbulent intensities of figure 4(*a*) can be replotted versus the dimensionless

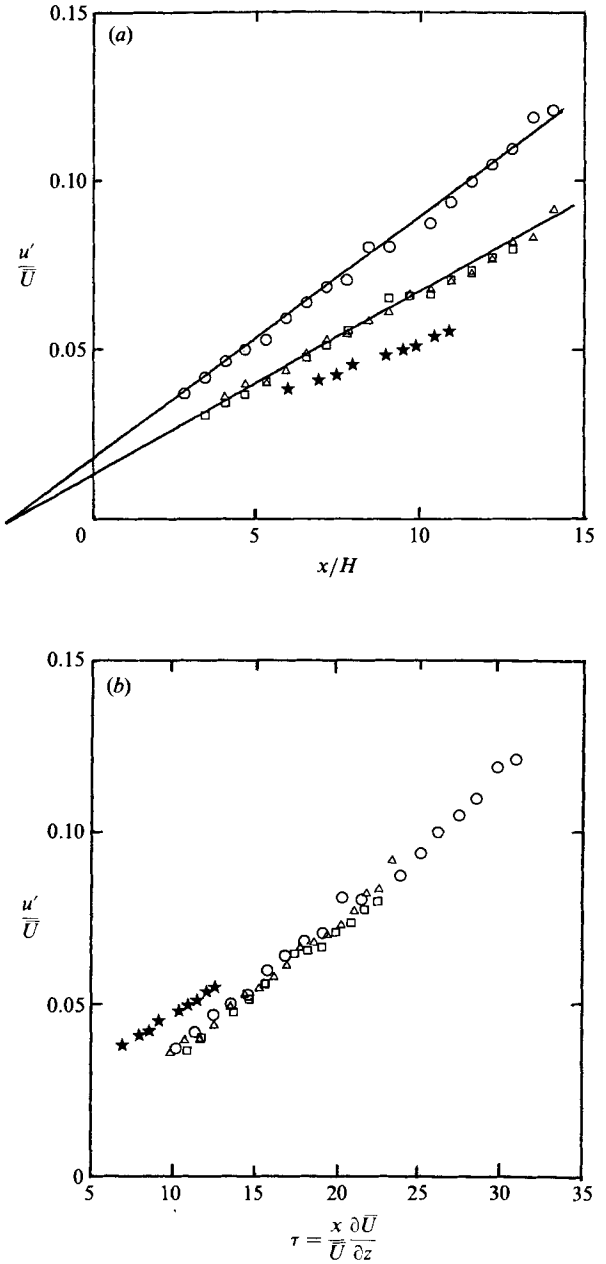

FIGURE 4. Longitudinal turbulent intensity as a function of (*a*) dimensionless downstream distance and (*b*) dimensionless development time.

	$\bar{U}$ (cm s^{-1})	$\partial\bar{U}/\partial z$ (s^{-1})	M (cm)	$-\tau_0$ (*b* only)
○	20.1	1.23	1.52	4.66
△	20.2	0.96	1.52	3.62
□	26.4	1.29	1.52	3.72
★ (TC)	1240	46.8	~ 1.5	

time $\tau = (x/\bar{U})\,(\partial\bar{U}/\partial z)$. The choice of this variable can be physically rationalized as follows (in the light of Tavoularis' work a more analytical development will be given in §6). If one assumes that to a first approximation the downstream rate of change of turbulent fluctuations scales with the mean shear, then, after integration, one would initially expect

$$\frac{u'}{\bar{U}} \approx c_1\left(\frac{x-x_0}{\bar{U}}\frac{\partial\bar{U}}{\partial z}\right) = c_1(\tau-\tau_0), \tag{16a}$$

$$\frac{w'}{\bar{U}} \approx c_2(\tau-\tau_0), \tag{16b}$$

$$\frac{v'}{\bar{U}} \approx c_3(\tau-\tau_0), \tag{16c}$$

where the c_i are independent of x. The downstream influence of the initial-disturbance lengthscales can be attributed solely to the x_0 (or τ_0) term, which determines a constant offset value of the turbulent intensity that persists throughout its downstream development. τ is the ratio of the flow convective timescale to the mean shear timescale and has appeared as a natural parameter in uniform-shear-flow studies (CHC; Mulhearn & Luxton 1975; HGC; TC). However, as will be seen from our experiments and the theoretical work of Tavoularis (1985), τ now assumes a much more fundamental role in characterizing the development of uniform-mean-shear flows.

Figure 4(*b*) demonstrates that $u'/\bar{U}$ grows at nearly the same rate regardless of the shear or the mean centreline velocity when growth is measured in terms of the dimensionless time τ. The reason for the collapse of the triangle and square data in figure 4(*a*) is because their values of $(\partial\bar{U}/\partial z)/\bar{U}$ happen to be similar ($\triangle$ = 0.048 cm^{-1}, $\bigcirc$ = 0.049 cm^{-1}), consequently x/H is proportional to $\tau = (x/U)\,(\partial\bar{U}/\partial z)$. The virtual origin x_0 estimated from figure 4(*a*) is subtracted from x to guarantee that at $\tau = 0$, $u'/\bar{U}$ will also equal zero. Adjusting for the virtual origin x_0 does not affect the growth rate of $u'/\bar{U}$ but provides an offset which facilitates comparison among different sets of data with identical inlet conditions. Also included in figure 4(*b*) are TC's data which, at least to a first approximation, have a similar dependence of $u'/\bar{U}$ on τ. This similarity is quite extraordinary considering that TC's mean velocity gradient and centreline velocity were about forty and sixty times greater, respectively, than that of our water-tunnel data. However, both experiments were within the same range of dimensionless time τ. HGC felt that attaining larger effective flow development times by lowering the mean speed would be outweighed by the desire for larger Reynolds number. Because the kinematic viscosity of water is about fifteen times smaller than that of air our grid Reynolds number ($U_c M/\nu \approx 3000$) is about one quarter of TC's, despite our much lower mean velocity. Our furthest downstream turbulent Reynolds number ($u'\lambda/\nu \approx 200$) is about 20% greater than TC's.

As previously mentioned (§2.2), although our flow initially is not as homogeneous as TC's, the major features of the developing flow become remarkably similar within a few τ. This observation is in agreement with Mulhearn & Luxton's (1975) conclusion that except for the initial specified disturbance lengthscale, the turbulence structure is practically independent of all other initial conditions. No attempt was made here to determine a virtual origin for TC's data.

Figure 5(*a*) shows the corresponding measurements for the vertical turbulent intensity $w'/\bar{U}$ with the same virtual origin as used for $u'/\bar{U}$. A different choice of

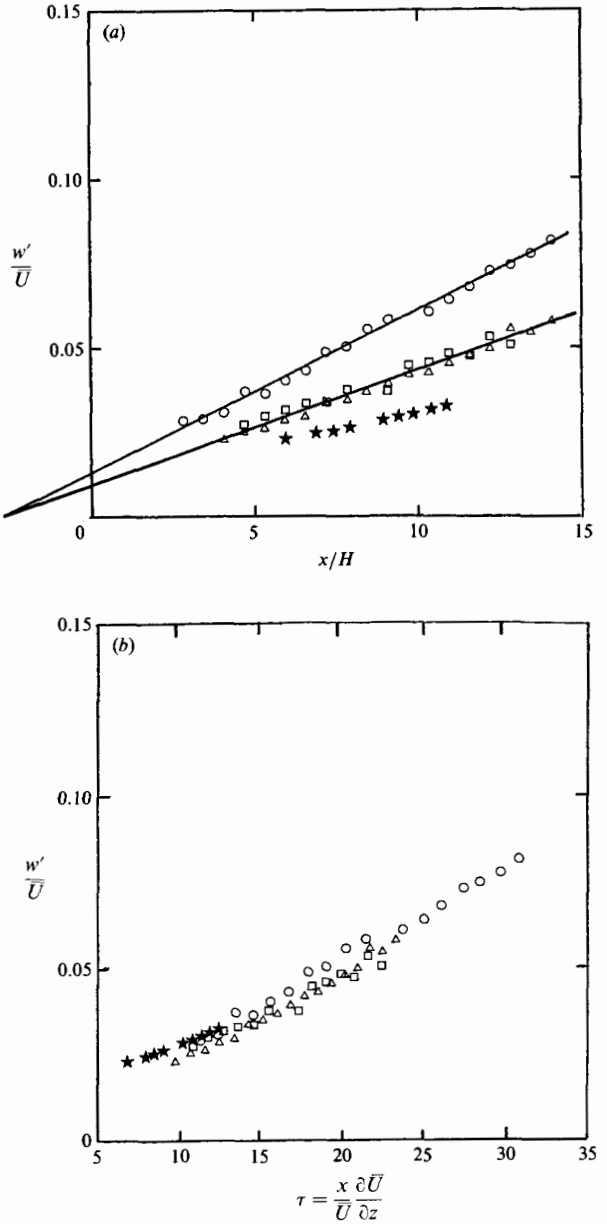

FIGURE 5. Vertical turbulent intensity as a function of (*a*) dimensionless downstream distance and (*b*) dimensionless development time. Symbols as for figure 4.

virtual origin for $w'/\bar{U}$ might give a better collapse for the data shown in figure 5(*b*). The ratio of the growth rates (slopes) of longitudinal and vertical turbulent intensities of figures 4(*a*) and 5(*b*) are found to be about 1.53 for either shear, which is fairly close to the ratio of 1.7 obtained by TC.

Rose (1970) investigated the effect of initial-disturbance lengthscales on the longitudinal turbulent intensity in the presence of a uniform mean shear. The initial disturbances were generated by grids of different mesh sizes but roughly equal solidity. In all his experiments both the centreline velocity and mean shear were kept

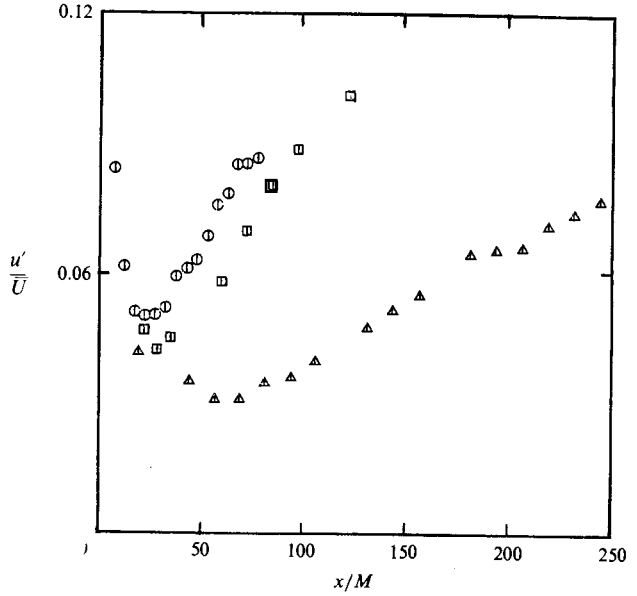

FIGURE 6. Longitudinal turbulent intensity as a function of dimensionless downstream distance (scaled with mesh size) for different initial-lengthscale disturbances.

	$\bar{U}$ (cm s^{-1})	$\partial\bar{U}/\partial z$ (s^{-1})	M (cm)
⊕	27.6	1.30	3.81 (grid)
⊞	20.4	1.13	3.05 (layer height)
△	26.4	1.20	1.52 (grid)

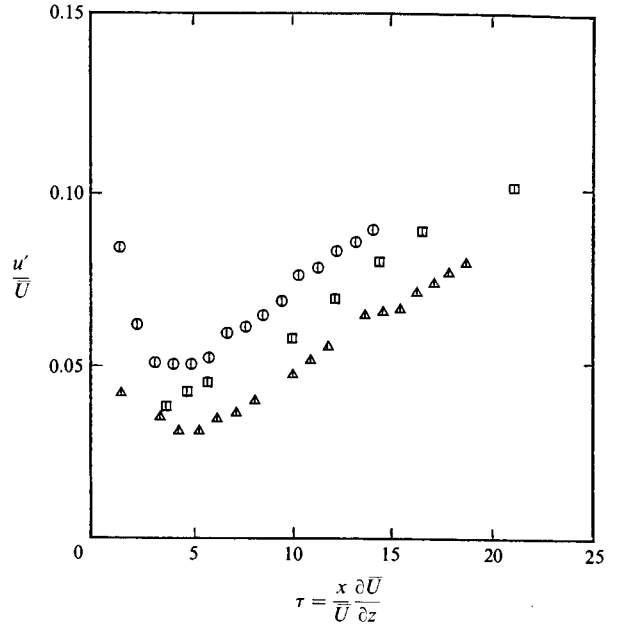

FIGURE 7. Longitudinal turbulent intensity as a function of dimensionless development time for different initial-lengthscale disturbances. Symbols as for figure 6.

nearly constant. Rose concluded from his measurements: '...that for a given value of mean shear the imposed length scale fixed in the energy level of the resulting turbulence, provided the scale is sufficiently large'. It has since been found by HGC, TC and KT that, when measurements are extended to large enough τ, the turbulence level does not remain fixed but monotonically increases. The present measurements can be used to determine how the initial lengthscale of the disturbance will affect the growth of turbulence at large development times.

Near the inlet to the test section where τ is small and the flow is grid dominated, the different turbulent-intensity data can be collapsed when they are plotted as a function of x/M. Batchelor & Townsend (1948) observed similar behaviour for the decay of grid turbulence in a uniform mean flow. More surprising is the continued downstream influence of the initial disturbance on the developing turbulence. This is best illustrated in figure 6 by comparing the data (⦶, ⧋) of similar mean velocity fields but different mesh size grids.

In figure 7 the previous values (figure 6) of $u'/\bar{U}$ are plotted as a function of τ. The effect of the different centreline velocities and mean shears on the rate of growth of $u'/\bar{U}$ is then, at least to a first approximation, accounted for. It is evident in figure 7 that increasing the initial-disturbance lengthscale results in an increasing offset in $u'/\bar{U}$ which persists downstream. When Rose's (1970, figure 6) data are plotted *vs.* τ the general behaviour is similar to the present data in the corresponding range of τ. As previously mentioned, Rose achieved only small values of $\tau (\tau < 4)$; consequently he observed no downstream growth in the turbulence intensities. Also included in figures 6 and 7 are measurements taken for a case with no grid at the inlet. Mulhearn & Luxton's (1975) results suggest that as the mean shear flow develops the details of the initial conditions become of minor importance apart from setting the initial scale of the disturbance. The initial scale characterizing the no-grid case will presumably be related to the height (3.05 cm) of the individual layers of the diffuser, and as expected from this argument the no-grid data set lies between the data sets of the 1.52 and 3.81 cm mesh grids. Similar offsets are observed for the vertical turbulent intensity.

These observations require that some previous conceptions be clarified. For example, KT stated that their observations confirm that '...the asymptotic turbulent structure depends on the shearing mechanism alone and that all initial-condition effects disappear downstream'. Although in the asymptotic region the turbulence may change at a rate independent of initial conditions, the absolute magnitude of the turbulent intensity is directly related to the magnitude of the initial disturbance. As long as the turbulence continues to interact with a constant mean shear, the data imply that the magnitude of the turbulent fluctuations should scale with the initial disturbance imposed at the inlet.

5. Comparison with wind-tunnel measurements

The results in §4 suggest that a more universal representation of the turbulence intensities developing in a uniform mean shear can be achieved if they are expressed as functions of τ. A crucial test of this hypothesis is whether these results can be applied to past wind-tunnel studies. Fortunately, the composite normalized turbulent-kinetic-energy data of KT and TC provide a good test over a large range of mean shear and centreline velocities. The data of figure 8 (*a*) were taken from figure 5 (*a*) of KT and figure 5 of TC. The only difference between the replotted and original

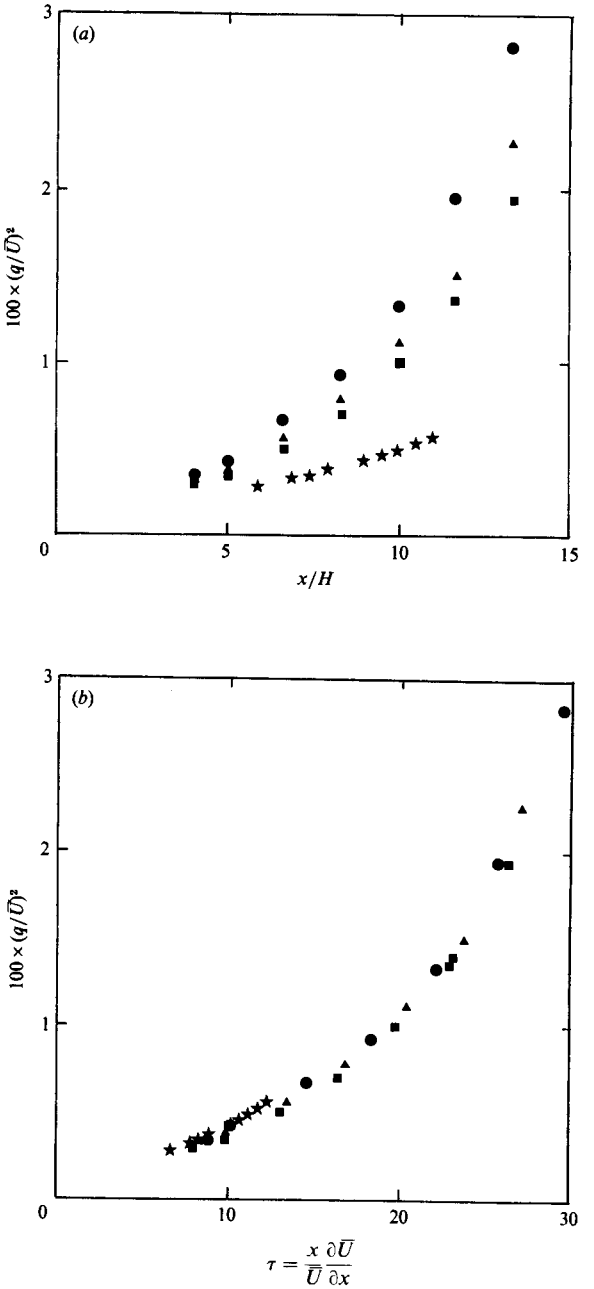

FIGURE 8. Normalized turbulent kinetic energy as a function of (*a*) dimensionless downstream distance (H = 1 ft) from TC and KT, and (*b*) dimensionless development time.

	$\bar{U}$ (cm s^{-1})	$\partial\bar{U}/\partial z$ (s^{-1})	
●	600	43.5	KT
▲	900	60.0	KT
■	1300	84.0	KT
★	1240	46.8	TC

data is that the coordinates in KT's figure 5(*a*) were semi-logarithmic while the present axes are linear to better test the quality of the collapse of the data.

KT's measurements were taken in a specially designed wind tunnel which was equipped with a shear generator that separated the flow into twelve channels. A system of interchangeable screens stretched across each channel provided the desired channel pressure drop. The values of the mean shear used in figure 8(*a*) were 43.5, 60 and 84 s^{-1} corresponding to centreline velocities of 6, 9 and 13 m s^{-1}, respectively. No other flow parameters were changed. Because the channels share a common air supply the adjustment of one channel affects the others, so the shear in this case could not be changed without changing the centreline velocity in the same proportion. KT remark that it is interesting that, although the value of $\bar{U}_c$ should not be a factor for determining the asymptotic turbulence structure, $\overline{q^2}$ shows almost universal values at any given downstream position when normalized with $\bar{U}_c^2$. The results of the present experiments (figures 4 and 5) offer an explanation for these observations. The ratios $(\partial\bar{U}/\partial z)/\bar{U}$ for the three turbulent-kinetic-energy curves of KT presented in figure 8(*a*) are 7.25, 6.67 and 6.46 m^{-1}, therefore KT's x-axis (x/H) is nearly proportional to $\tau = (x/\bar{U})(\partial\bar{U}/\partial z)$. In the light of our results this fact could be responsible for KT's observation of almost universal $\overline{q^2}/\bar{U}^2$ values. If this reasoning is correct, then by replotting figure 8(*a*) explicitly as a function of τ, a better collapse of KT's data should be achieved. Figure 8(*b*) shows that an excellent collapse of the KT data is indeed obtained. It was checked whether this collapse would be adversely affected if the virtual-origin corrections were included. Replotting KT's data as $(\overline{q^2})^{\frac{1}{2}}/\bar{U}$ *vs.* x/H and extrapolating, a common virtual origin was found. When this common virtual origin (x_0) is multiplied by the appropriate value of $(\partial\bar{U}/\partial z)/\bar{U}$ for each curve and the resulting offset is included in figure 8(*b*), very little effect is noted on the collapse of those data because x_0 is found to be small (< 1) and $(\partial\bar{U}/\partial z)/\bar{U}$ is almost the same for each curve.

In figure 8(*a*) the data of KT at a centreline speed of 6 m s^{-1} and a mean shear of 43.5 s^{-1} can be compared to the data of TC at a centreline speed of 12.4 m s^{-1} and a mean shear of 46.8 s^{-1}. As for the water-channel measurements (figure 4*a*) the turbulence is observed to grow faster for the smaller centreline velocity, given that the mean shear is about the same. One final comparison can be made. The measurements taken by KT at a centreline speed of 13 m s^{-1} and a mean shear of 84 s^{-1} are shown by the squares in figure 8(*a*). While 13 m s^{-1} is very close to the centreline velocity of 12.4 m s^{-1} used by TC, TC's mean shear of 46.8 s^{-1} is substantially smaller. Again, as anticipated from water-channel measurements, for almost equal centreline velocities the turbulent kinetic energies increase much faster downstream (x/H) for the larger shear.

When plotted against τ in figure 8(*b*) the growth curves of KT and TC from figure 8(*a*) collapse reasonably well, corroborating the results from the present water-channel experiments. No correction has been made for the different virtual origins of KT and TC though presumably an even better collapse of the measurements would result if this were done. It should be noted that when Tavoularis (1985, figure 1) plotted the log of these same data $\overline{q^2}$ was non-dimensionalized with $\overline{q^2}$, which is quite different for the two experiments. However, the difference in slope found by Tavoularis between the TC and KT data (which were taken in different facilities) cannot be accounted for by different $\overline{q_r^2}$. Discrepancy is exhibited in figure 8(*b*) by the slightly different shapes of the TC and KT measurements.

6. Comparison with the asymptotic law of Tavoularis (1985)

The previous success in collapsing turbulent-intensity measurements in uniform-mean-shear flows as a function of τ, suggests that a fundamental connection between τ and the governing equations should exist. Tavoularis (1985) proposed a semi-analytical analysis for such flows which predicts a weak exponential downstream growth of the turbulent kinetic energy. Tavoularis' (1985) prediction is found to be in good agreement with the experimental results of KT. As previously discussed this prediction is shown to be independent of Tavoularis' assumption that the dissipation but not the production term in the approximate turbulent-kinetic-energy equation (11) is dependent on z. Assuming (11) is a good approximation, as indicated by the measurements of HGC and TC, then it is only necessary that $\overline{uw}/\overline{q^2}$, $\partial\bar{U}/\partial z$ and ϵ/P are independent of x. In principle, as discussed by Hinze, this cannot be strictly true. For example $\partial\bar{U}/\partial z$ must decay downstream, as it is the exclusive source for the downstream turbulent growth. However, the downstream variations of $\overline{uw}/\overline{q^2}$, $\bar{U}$ and $\partial\bar{U}/\partial z$ have been found experimentally to be small by HGC, TC, and KT.

None of the previous wind-tunnel experiments have measured ϵ directly, arguing instead that a better approximation can be arrived at by balancing the other two terms in (11). We estimated the dissipation from the one-dimensional spectrum using isotropic relations.† Figure 9 presents the ϵ and P measurements corresponding to figure 4. It is seen that after the influence of the grid diminishes, the constant slopes of ϵ and P as a function of x imply that the ratio of the production to the dissipation approaches a constant for large x. The asymptotic values of ϵ/P for the wind-tunnel data in figure 8 with nearly the same centreline velocity are listed by KT (their table 1) as 0.71 for their high-shear case (■) and 0.57 for the low-shear case of TC. This observed dependence of ϵ/P on shear for nearly the same $\bar{U}$ is opposite to what one might expect. If with increasing mean shear ϵ grows faster than P, by (11) the rate of growth of turbulence must decrease with increasing shear, clearly in contradiction to what is observed (figure 8*a*). More reasonable is the asymptotic ratio of ϵ/P for the water-channel data. In figure 9 (for nearly the same $\bar{U}$) ϵ/P is about 0.6 for the high shear and about 0.9 for the low shear. Although this decrease of ϵ/P with increasing shear and turbulence growth is also consistent with what HCG found after increasing the shear of CHC, CHC's flow field had not yet reached an asymptotic state. It is also possible that ϵ/P is independent of mean shear but that neither the water nor the wind-tunnel measurements are accurate enough to determine this.

Rearranging (13) Tavoularis' exponential solution may be rewritten:

$$\overline{q^2} = \overline{q_r^2}\exp\left\{\left(\frac{x_1-x_r}{\bar{U}}\frac{\partial\bar{U}}{\partial z}\right)\left[\frac{-\overline{uw}}{q^2}2\left(1-\frac{\epsilon}{P}\right)\right]\right\}, \tag{17}$$

where $[(x_1-x_r)/U]\,(\partial\bar{U}/\partial z)$ is τ_r measured from some point x_r at the beginning of the asymptotic range. Taking the square root of both sides of (17) and expanding the exponential:

$$(\overline{q^2})^{\frac{1}{2}} = (\overline{q_r^2})^{\frac{1}{2}}\left\{1+\tau_r\left[\frac{-\overline{uw}}{\overline{q^2}}\left(1-\frac{\epsilon}{P}\right)\right]+\tau_r^2\left[\frac{-\overline{uw}}{\overline{q^2}}\left(1-\frac{\epsilon}{P}\right)\right]^2+\ldots\right\}. \tag{18}$$

† The isotropic relation $\epsilon = \nu[10\overline{(\partial u/\partial x)^2}+2.5\overline{(\partial w/\partial x)^2}]$ has been used, where $\overline{(\partial u/\partial x)^2}$ and $\overline{(\partial w/\partial x)^2}$ are calculated by integrating k^2 times the one-dimensional energy spectra of $E_{uu}(k)$ and $E_{ww}(k)$ respectively. TC had found for uniform-mean-shear flows that $\epsilon \approx 8.5(\overline{q^2}/\overline{u'^2})$ or since $\overline{q^2} \approx 1.89\,\overline{u'^2}$, $\epsilon \approx 16.07\,\nu\overline{(\partial u/\partial x)^2}$. They also found that $\overline{(\partial w/\partial x)^2} \approx 2.6\overline{(\partial u/\partial x)^2}$ so that the isotropic relation for the dissipation can be rewritten as $\epsilon \approx 16.5\,\nu\overline{(\partial u/\partial x)^2}$, which is close to TC's estimate for the uniform mean shear case.

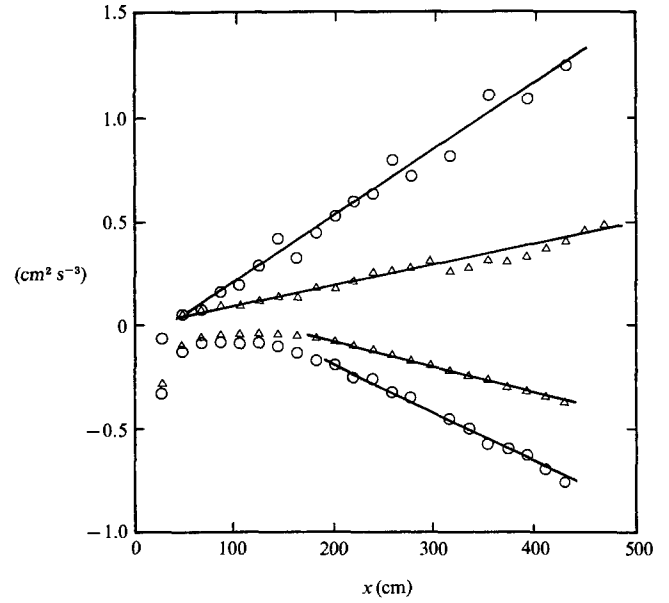

FIGURE 9. Turbulence production P (greater than zero) and negative dissipation ϵ (less than zero) as a function of distance downstream.

	$\bar{U}$ (cm s^{-1})	$\partial\bar{U}/\partial z$ (s^{-1})	M (cm)
○	20.1	1.23	1.52
△	20.2	0.96	1.52

The first two terms in the expansion are similar to the previous solution (16); higher terms then act as corrections to the original hypothesis.

The term $(-\overline{uw}/\overline{q^2}\,(1-\epsilon/P)$ has been tabulated by KT (their table 1) for a number of wind-tunnel experiments from different facilities and was found to be very small but not necessarily constant between experiments. In particular for KT's measurements it was estimated to be about 0.046. The higher-order terms in the exponential expansion, especially for small τ_r, can often then be neglected. This is entirely consistent with the apparent linear growth of the turbulent intensities with small τ (or the quadratic growth of $\overline{q^2}/\bar{U}^2$ with τ) as presented in figures 4–8. When the turbulent intensities of figures 4 and 5 are plotted in semi-logarithmic coordinates *vs.* x/H a weak exponential growth may also be inferred.

With identical inlet conditions KT found nearly the same asymptotic centreline value of $(-\overline{uw}/\overline{q^2})\,(1-\epsilon/P)$ regardless of the value of $\bar{U}_c$ or $\partial\bar{U}/\partial z$. The collapse of the water-channel turbulent-intensity data as a function of τ for identical inlet conditions also suggests that $(-\overline{uw}/\overline{q^2})\,(1-(\epsilon/P))$ approaches a constant asymptotic value independent of the mean centreline velocity and the uniform mean shear. However, how $(-\overline{uw}/\overline{q^2})\,(1-(\epsilon/P))$ changes from facility to facility is not understood. We have found that, in addition to the size of the entrance grid mesh, the distance between the grid and the inlet can also introduce an offset in the turbulent intensity *vs.* τ curve. As seen in figure 10 (note that $\tau = 0$ corresponds to the position of the grid) decreasing this distance results in a positive offset. This offset cannot be accounted for by including the different virtual origins. For this particular flow a 10 cm separation distance between grid and inlet results in a very small change in $\tau(\approx 0.1)$.

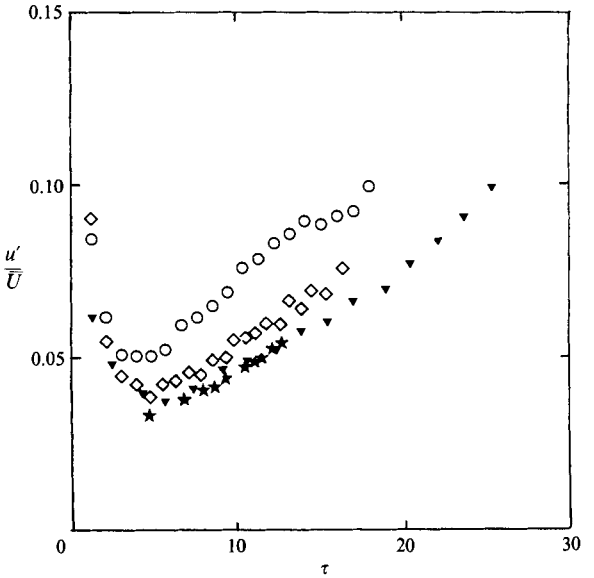

FIGURE 10. Measurements from different facilities and inlet configurations of the longitudinal turbulent intensity as a function of dimensionless development time.

			M	
	$\bar{U}$ (cm s^{-1})	$\partial\bar{U}/\partial z$ (s^{-1})	Size (cm)	Location (x/H)
○	27.6	1.30	3.81	~ 0.03
◇	28.0	1.21	3.81	0.3
▼ (KT)	1300	84	~ 2.54 (layer height)	0
★ (TC)	1240	46.8	~ 1.5	0

When separation distances result in large changes in τ the trends exhibited in figure 10 may not continue; at least this was found for the KT data where the equivalent change in τ was ≈ 2.8 and ≈ 3.4.

In the asymptotic region of turbulent growth the slope of the turbulent intensity *vs.* τ curve seems more dependent on how quickly the mean velocity profile is decaying. In our preliminary experiments we have found cases where the erosion of the mean velocity gradient was severe enough eventually to arrest turbulent growth. Figure 10 illustrates some of the different initial slopes of $u'/\bar{U}$ *vs.* τ associated with measurements taken from different facilities. Where the turbulence is growing the slopes of $u'/\bar{U}$ *vs.* τ are found not to differ greatly. A need for further observations is necessary before a clearer interpretation can be achieved.

Whereas τ_r clearly exhibits a strong z-dependence, it is not known how $(\overline{q_r^2})^{\frac{1}{2}}[-(\overline{uw}/\overline{q^2})(1-(\epsilon/P))]$ depends on z. If the z-dependence of τ_r prevails then (18) predicts for large τ that $(\overline{q^2})^{\frac{1}{2}}$ should grow downstream unevenly along the mean shear flow, increasing faster with smaller values of $\bar{U}(z)$. Figure 3(*b*) shows such a trend for both the water-channel and TK measurements which are taken at the highest values of τ to date. These trends were restricted to the central positon of the flow where the mean shear was nearly uniform. A possible mechanism for this vertical inhomogeneity is that turbulent structures, moving at a smaller mean velocity in the lower part of the flow, interact with the mean shear over a longer time than structure higher up moving at greater velocities. This observation, that the growth of u' is

dependent on $\bar{U}(z)$, is equivalent to that drawn from figure 4(*a*) (○, □) but now, instead of changing the entire mean velocity field keeping $\partial\bar{U}/\partial z$ constant, the measurement locations are simply moved along the direction of the mean shear. It is these measurements which are most persuasive since they were taken where the mean velocity profile was least affected by boundary-layer growth. Furthermore, as previously seen in figure 8(*a*) (○, ★), similar wind-tunnel measurements are in agreement. In the central regions of the mean profiles where the mean strain remained uniform, the Reynolds shear stress exhibited similar trends, i.e. increasing with decreasing z. An increase in turbulent production in the direction of decreasing mean velocity is consistent with wind-tunnel observations (see TC; Tavoularis 1985) of a corresponding increase in dissipation.

These results imply that turbulence in uniform shear flows cannot remain homogeneous along the direction of the mean shear. Although previous wind-tunnel investigations (HGC; TC) have found vertical inhomogeneity in the Taylor microscale similar inhomogeneities in u' and $\overline{uw}$ have not been generally accepted. As previously mentioned, in comparison to wind-tunnel work, the inhomogeneities in the water channel are thought to be greater because of the quicker decay of the mean velocity profile. Nevertheless water-channel measurements predict that two series of downstream measurements of wind-tunnel velocity fluctuations, separated along the mean shear, will diverge owing to an increasing difference in τ.

7. Downstream development of lengthscales and spectra

Figure 11 compares the evolution of the characteristic lengthscales for uniform-gradient shear flows (designated by symbols) and unsheared grid-generated turbulence (designated by a solid line) experiments. Except for the TC wind-tunnel data, the data shown were taken in the UCSD water channel.

The Kolmogorov scale, $L_k = (\nu^3/\epsilon)^{\frac{1}{4}}$, is a measure of the smallest turbulent lengthscales. If there is no source of turbulence, ϵ must continually decrease and consequently L_k will grow monotonically. As expected, for the uniform-mean-velocity case L_k grows continually downstream as the turbulence decays (solid line). For the present shear experiments we find that at small x_1, where the flow is grid dominated ($x < 100$) the turbulence initially decreases behind the grid and L_k is consequently observed to increase initially downstream. Further downstream, however, where the flow is shear dominated ($x > 100$) L_k monotonically decreases as the energy provided by the growing production term is first transferred to increasingly larger scales and subsequently to smaller scales. The downstream decrease in L_k is corroborated by the horizontal and vertical velocity power spectra. In figures 13 and 14 these spectra are found to include smaller scales with increasing downstream distance for data taken in the shear-dominated region of the flow. Presumably the larger the mean shear (and assuming all other parameters remain the same) the smaller L_k should be, which is observed in figure 11. The L_k measurements of TC are found to behave similarly to the present measurements.

The Taylor microscale λ is also shown in figure 11. λ is inferred for the uniform-mean-flow case from the isotropic relation $\epsilon = 10\,\nu\overline{q^2}/\lambda^2$. For the uniform-gradient shear flows λ is inferred from the experimental relation $\epsilon = 8.5\,\nu\overline{q^2}/\lambda^2$ (Tavoularis 1985). Although λ does not characterize any specific group of eddies, λ^{-2} may be thought of as the mean-square wavenumber of sinusoidal velocity fluctuations weighted according to their contribution to the total energy (Batchelor & Townsend 1948). For the case of uniform mean velocity (solid line), energy at all scales is

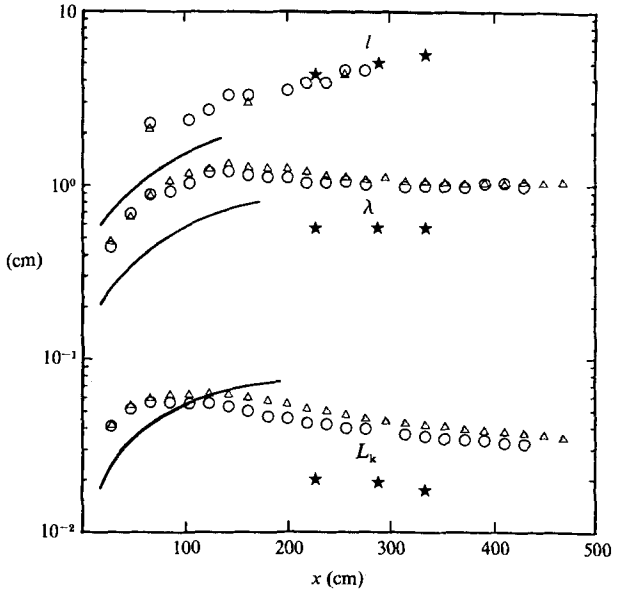

FIGURE 11. Downstream development of characteristic lengthscales.

	$\bar{U}$ (cm s^{-1})	$\partial\bar{U}/\partial z$ (s^{-1})	M (cm)
○	20.1	1.23	1.52
△	20.2	0.96	1.52
★ (TC)	1240	46.8	~ 1.5
—	25.5	0	1.905

decaying, but because the smaller scales decay faster than large scales, the Taylor microscale grows monotonically. In the uniform-shear case, close to the grid where the influence of the grid is large and the flow development time (τ) is small, λ is observed to increase initially, in agreement with the observations of CHC for small τ. The uniform-mean-flow values of L_k and λ are smaller than the corresponding shear values taken close to the grid because of the higher centreline values of the former (25 cm s^{-1} as opposed to 20 cm s^{-1}). For larger τ, λ is observed to remain nearly constant for both the water- and wind-tunnel uniform-gradient shear measurements.

The integral lengthscale l is a measure of the largest scale of motion in the flow. TC found that the integral lengthscales computed from their spectra were not appreciably different from those computed from velocity correlations. The integral scales in figure 11 were all computed by extrapolating the one-dimensional energy spectra to zero frequency, but because of the limited record length of the water-channel measurements, this estimate could not be relied on for large x/M† where the scales are too large to be spectrally resolved. As the integral scale grows, while the record time remains fixed, it becomes increasingly difficult to ascertain where the one-dimensional spectra are levelling off. The reasons for the growing integral scales of the sheared and unsheared flows of figure 11 are very different. The integral scale l is proportional to $(1/\overline{u^2})\lim_{f\to 0} E_{uu}(f)$. In the unsheared flow l grows downstream

† For the larger grid mesh size l is found initially to be sufficiently large that, owing to the limited record length of water-channel measurements, reliable estimates were precluded even for small values of τ.

because $\overline{u^2}$ decreases downstream faster than $\lim_{f\to 0} E_{uu}(f)$. In the sheared flow, however, $\overline{u^2}$ grows downstream, therefore l increases owing to the faster growth of $\lim_{f\to 0} E_{uu}(f)$. This implies that the absolute size of the largest eddies, as reflected by the spectra, are growing only in the shear-flow case.

The similarity of the growth of the integral scale as a function of x between the three sets of data presented in figure 11 is somewhat surprising. Our experience with the corresponding turbulent intensities might suggest that the data should assume similar form only as a function of τ. The ratios of $\partial\bar{U}/\partial z$ to $\bar{U}$ for the three experiments differ by as much as 60% (0.0377, ★; 0.0475, △; and 0.0612 cm^{-1}, ○) so that the same data plotted *vs.* τ would result in three clearly distinct lines. HGC were similarly surprised when they compared their measurements to CHC's and discovered that the two sets of integral-scale data seemed to be independent of the mean strain rate. In their comparison, where the facility, inlet conditions and centreline velocity were identical, the mean shear of HGC was nearly four times that of CHC. A possible criticism of this comparison is that the velocity field of CHC had not reached its asymptotic state. This objection does not necessarily preclude the possibility that the integral scales had reached their final state of growth, because not all the features of the turbulence are observed to evolve at the same rate. In figure 9 the production term appears to have settled into its asymptotic growth much sooner than the dissipation term. KT's data were all taken in the asymptotic range and they also observed that the integral lengthscales developed independently of the values of the mean shear and centreline velocity. While it has been shown (figure 8*b*) that KT's velocity measurements collapse significantly better when plotted *vs.* τ, this is not found to be true for the corresponding integral scales. As seen in figure 12, when the data of figure 11 are replotted in linear–linear coordinates, an equally good linear dependence is found, Included in figure 12 are integral scales of HGC and KT. It should be noted that the poor linear fit of the KT data shown in figure 12 is not improved when plotted in semi-logarithmic coordinates (see figure 7*a* of KT).

If the larger eddies maintain their vorticity through interactions with the mean shear as Tennekes & Lumley (1972) suggest, then

$$\frac{w'}{l} = C_3 \frac{\partial \bar{U}}{\partial z}. \tag{19}$$

If (16*b*) and (19) are both correct, l must grow independently of the mean shear and linearly with $(x-x_0)$, where x_0 is an offset dependent on the initial-disturbance lengthscale. Equation (19) is similar to the simple mixing-length type of proportionality proposed by Prandtl (1925); i.e. $u' = C_4 l(\partial\bar{U}/\partial z)$. In table 1 the proportionality constant C_4 is calculated for the integral lengthscales shown in figure 11 and found to be roughly constant for experiments which all share similar initial-disturbance lengthscales. Although the phenomenological model of a mixing length (in analogy with the mean free path in the kinetic theory of gases) must be rejected, mixing-length expressions like (19) make good dimensional sense in situations where only one lengthscale and timescale are relevant (see Tennekes & Lumley 1972).

Figures 13 and 14 show representative velocity spectra corresponding to the uniform-mean-sheared water-channel data of figures 4 and 5. Beyond the grid-influenced region ($x/M > 80$) both the longitudinal (figure 13) and vertical (figure 14) one-dimensional velocity spectra monotonically increase at all frequencies with increasing downstream location.

Figures 15 and 16 illustrate how well these one-dimensional longitudinal velocity spectra tend to collapse to a single universal curve when normalized by the

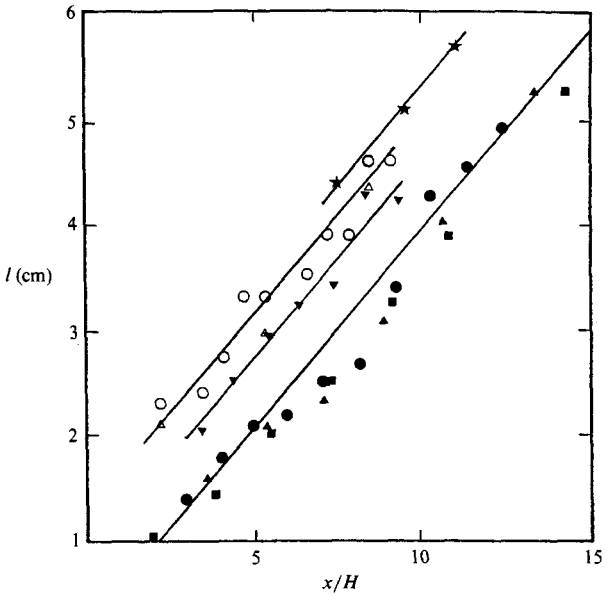

FIGURE 12. Downstream development of integral length scales ($H \approx 30.5$ cm for all experiments).

	$\bar{U}$ (cm s^{-1})	$\partial\bar{U}/\partial z$ (s^{-1})	M (cm)
○	20.1	1.23	1.52
△	20.2	0.96	1.52
★ TC	1240.0	46.8	~ 1.5
▼ HGC	1240.0	46.8	~ 1.5
●	600.0	43.5	
▲ KT	900.0	60.0	~ 2.54 (layer height)
■	1300.0	85.0	

	$\frac{x}{H}$	$l\frac{\partial\bar{U}}{\partial z}$ (m s^{-1})	u' (m s^{-1})	$1/C_4 = l\frac{\partial\bar{U}}{\partial z}\Big/u'$	
TC (★) (their table 4)	7.5	2.06	0.529	3.89	
	9.5	2.39	0.616	3.87	3.88±0.01
	11	2.67	0.689	3.88	
HGC (their table 3)	11	2.54	0.641	3.97	
Water channel (○)	2.5	0.0295	0.0084	3.51	
	3	0.0337	0.0096	3.49	
	3.5	0.0408	0.01056	3.86	
	4	0.0408	0.01133	3.60	3.50±0.18
	5	0.0434	0.01328	3.26	
	6	0.0428	0.01442	3.31	
	6.5	0.0566	0.01637	3.46	
	7	0.0566	0.01602	3.53	
Water channel (△)	4	0.0303	0.00842	3.53	3.61±0.11
	6.5	0.0405	0.0179	3.69	

TABLE 1. Comparison of Prandtl's mixing-length proportionality constant, $1/C_4 = l(\partial\bar{U}/\partial z)/u'$, for different experiments. Symbols correspond to figure 11.

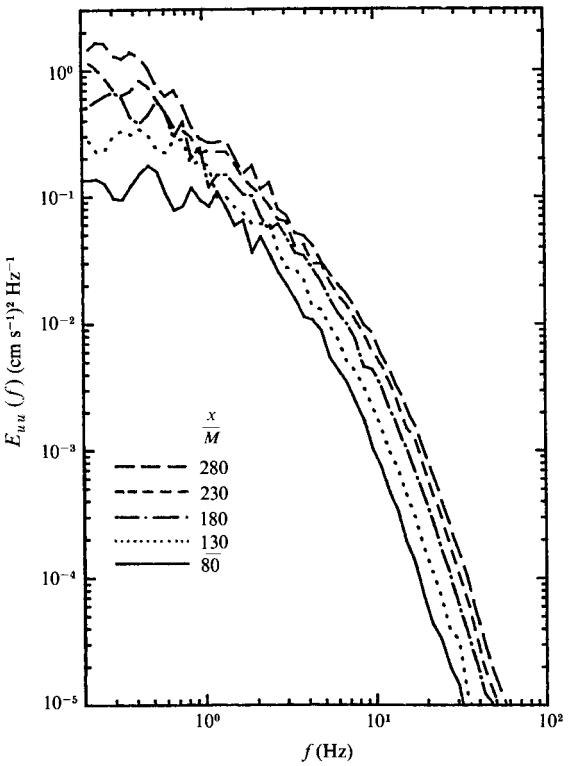

FIGURE 13. One-dimensional spectra of the longitudinal turbulent velocity.

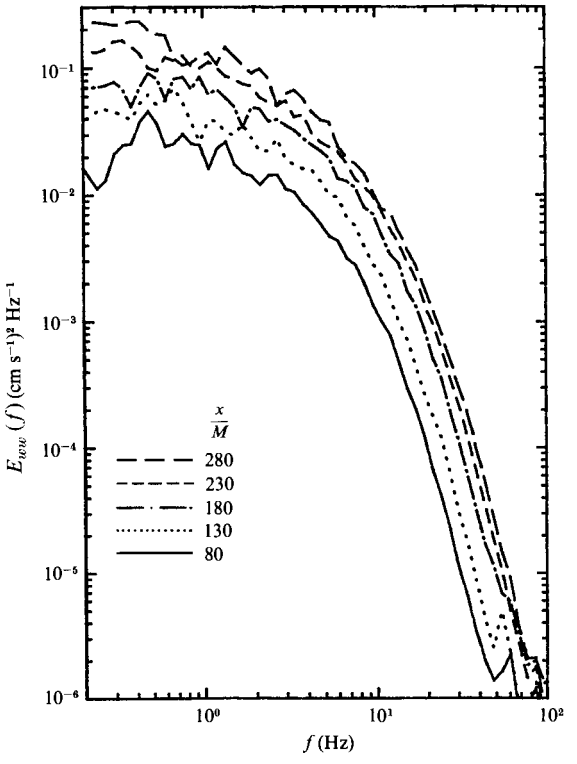

FIGURE 14. One-dimensional spectra of the vertical turbulent velocity.

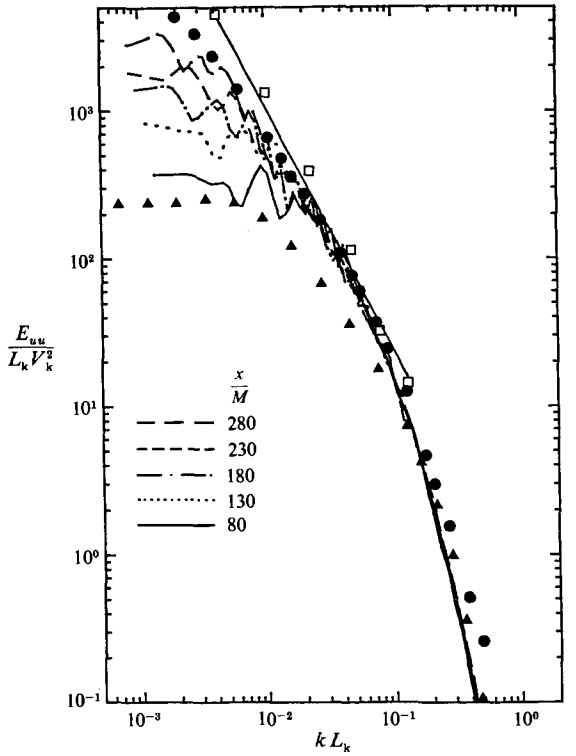

FIGURE 15. Normalized one-dimensional turbulent longitudinal velocity spectra. □–□, Grant, Stewart & Moilliet (1962); ●, TC; ▲, Helland, Lii & Rosenblatt (1977).

Kolmogorov scales. For the present data there has been no attempt to correct the higher frequencies for the finite sensor length. Included also in figures 15 and 16, for the sake of comparison, are the normalized velocity spectra from some very different turbulent flows. The agreement among the spectra is reasonably good as required by Kolmogorov universal similarity, but some deviations do exist because of the finite sensor length.

The data represented by the solid circles in figure 15 were derived from the Tavoularis & Corrsin (TC, figure 16) uniform-shear spectrum. These data, taken at $x/h = 10.5$, were normalized by the appropriate ϵ- and ν-values listed in table 4 of TC. The spectra were then divided by two because of the different definitions of $E_{uu}(k_1)$, i.e. for the present water-channel data

$$\int_0^\infty E_{uu}(k_1)\,\mathrm{d}k_1 = (\tfrac{1}{2}\overline{u^2}),$$

while TC use

$$\int_0^\infty E_{uu}(k_1)\,\mathrm{d}k_1 = \overline{u^2}.$$

TC's measurements were taken in a wind tunnel with a mean velocity gradient of 46.8 s^{-1} and centreline velocity of 1240 cm s^{-1}. The turbulent Reynolds number $(u'\lambda/\nu)$ was 160. The square symbols in figure 15 are taken from figure 6.2 of Phillips (1966), which is simply a composite of the Kolmogorov-scaled spectra appearing in the original paper by Grant, Stewart & Moilliet (1962, figures 12 and 13). These spectral values were also divided by two in order to achieve consistent definitions

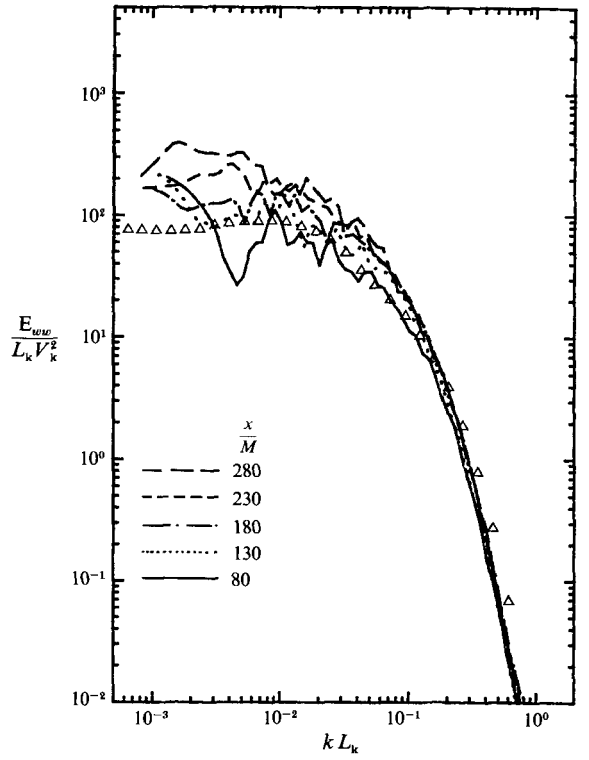

FIGURE 16. Normalized one-dimensional turbulent vertical velocity spectra. △, Helland, Lii & Rosenblatt (1977).

of $E_{uu}(k_1)$. The higher-wavenumber part of this spectrum is deleted because of instrumentation noise problems (see Grant *et al.* 1962). The Reynolds number of the oceanic measurements based on the mean flow and depth of the tidal channel is around 10^8. The data denoted by triangles in figures 15 and 16 represent measurements of decaying grid turbulence taken in a wind tunnel by Helland, Lii & Rosenblatt (1977), where the grid Reynolds number ($\bar{U}M/\nu$) is about 26000 while the turbulent Reynolds number ($u'\lambda/\nu$) is around 35. A line of slope-$\frac{5}{3}$ is also included to show how the developing spectra approach the inertial subrange.

The lined data (solid, dashed, etc.) in figures 15 and 16 are the corresponding spectra of figures 13 and 14 when normalized by the appropriate Kolmogorov length- and velocity scales. The grid Reynolds number is 3000 whereas the turbulent Reynolds number ranges from about 100 to 200, increasing downstream with u', while λ remains nearly constant (see figure 11). The tendency for the water-channel shear spectra to approach the universal equilibrium spectrum with increasing τ (or x since $\tau = (x/\bar{U})\,(\partial\bar{U}/\partial z)$) is apparent. It may be at first surprising that in figure 15 the Kolmogorov-scaled shear spectra with a smaller mean-flow Reynolds number ($\bar{U}M/\nu$) than the similarly scaled grid data (△), exhibit a significantly greater portion of the universal spectrum; however, the turbulent Reynolds number ($u'\lambda/\nu$) of the former was much larger than the latter.

8. Implications of τ in interpreting other shear-flow phenomena

If τ is accepted as a fundamental parameter of uniform-mean-shear flows, a simpler interpretation of some other past experimental results can be obtained. As a first example, consider KT's attempt to establish an experimental stability criterion for uniformly shear flows using Hasen's (1967) stability analysis. Hasen's analysis, which considers finite two-dimensional eddy fluctuations in viscous incompressible flows, predicts that there exists a stability barrier for the initial amplitude of the eddy fluctuations that can be expressed as

$$\left(\frac{1}{L}\frac{\partial \bar{U}}{\partial z}\right)^{\frac{1}{3}} \nu^{\frac{2}{3}} k_2 \leqslant u_{\mathrm{b}} \leqslant \left(\frac{1}{L}\frac{\partial \bar{U}}{\partial z}\right)^{\frac{1}{3}} \nu^{\frac{2}{3}} k_1, \tag{20}$$

where L is the lengthscale of the initial eddies. If the initial amplitude of the eddy fluctuations is less than u_{b} then the fluctuations decay as $\tau \to \infty$ and if they are larger the energy of the fluctuations does not decay. KT computes $[(1/L)(\partial \bar{U}/\partial z)]^{\frac{1}{3}} \nu^{\frac{2}{3}}$ for flows where q^2 is observed to grow (TC; KT) and for those where $\overline{q^2}$ only reaches a constant value (CHC; Rose 1966, 1970; Mulhearn & Luxton 1975; KT). They find that $\overline{q^2}$ is observed to grow only when $[(1/L)(\partial \bar{U}/\partial z)]^{\frac{1}{3}} \nu^{\frac{2}{3}} \geqslant 4.5$ mm s^{-1} and reaches a constant asymptotic state for $3 < [(1/L)(\partial \bar{U}/\partial z)]^{\frac{1}{3}} \nu^{\frac{2}{3}} < 4.5$ mm s^{-1}.

There are several difficulties with Hasen's and KT's use of $[(1/L)(\partial \bar{U}/\partial z)]^{\frac{1}{3}} \nu^{\frac{2}{3}}$ as a criterion for stability: when it is calculated for the present water-channel measurements, where the downstream growth of $\overline{q^2}$ is unmistakable, it is found to be an order-of-magnitude smaller than KT's stability barrier of 4.5 mm s^{-1}. Also for both Rose's (1970) and the present measurements there is no sign of promoting the decay of turbulence by increasing the initial-disturbance lengthscale as KT have found and (20) suggests. Finally, in all the measurements that KT compared, the integral scales were always observed to grow regardless of their u_{b} value. CHC were the first to recognize that in the presence of a constant mean velocity gradient, growing integral scales should lead to a growth in the turbulent kinetic energy. They suggested that a growth in $\overline{q^2}$ might have been observed in their own data if it were not for the small flow development times. HGC confirmed CHC's insight by observing a growth in $\overline{q^2}$ at larger dimensionless development times $\tau(\tau > 4)$. Although HGC increased τ by increasing $\partial \bar{U}/\partial z$, it has been shown in the previous sections that τ can also be increased by decreasing $\bar{U}$ or increasing x. These later methods would provide larger τ-values without changing u_{b}.

The development of $\overline{q^2}$ in a turbulent uniform mean shear can be explained much more simply in terms of τ. Whether $\overline{q^2}$ is constant, decaying or growing becomes a question of whether there is enough dimensionless time for fluctuations to grow above the background noise, rather than a question of stability. In all the uniform-mean-shear flows that have been investigated, the turbulent kinetic energy always decreases immediately behind the grid. Near the inlet the fluid has not had enough time to react to the mean shear. Therefore as long as the production term is small compared with the dissipation rate, the flow is mostly characteristic of a decaying grid turbulence. If measurements were restricted to these small values of τ, they would erroneously suggest that the turbulence should continue to decrease downstream. Similarly, the fact that $\overline{q^2}$ was observed to approach a constant value at some location does not necessarily imply that it will remain constant at further downstream positions. The region where $\overline{q^2}$ is a constant occurs when the shear production just compensates for the loss of turbulent kinetic energy of the initial grid decay. The exact value of τ where this balance occurs will presumably depend on the

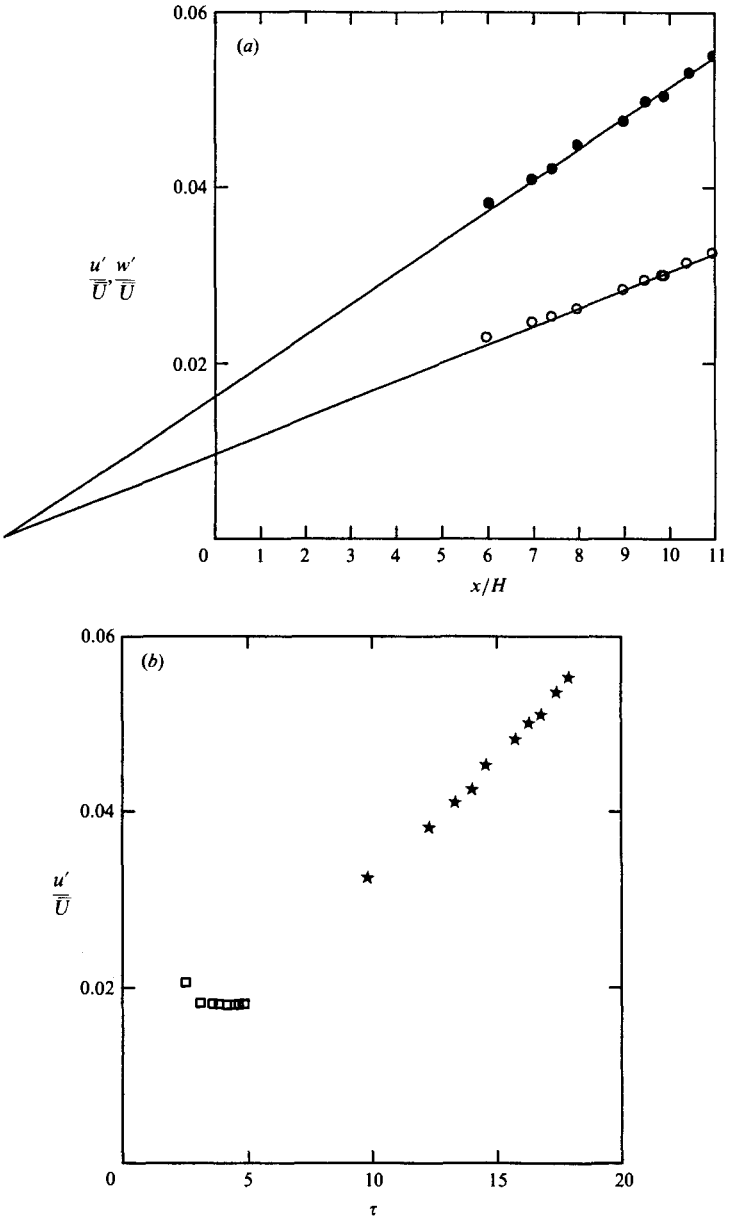

FIGURE 17. (*a*) Longitudinal (●) and vertical (○) turbulent intensity as a function of dimensionless downstream distance; from TC. (*b*) Longitudinal turbulent intensity as a function of dimensionless time.

		$\overline{U}$ (cm s^{-1})	$\partial\overline{U}/\partial z$ (s^{-1})	M (cm)	$-\tau_0$
□	Champagne, Harris & Corrsin (1970)	1240	12.9	~ 1.5	1.46
★	TC	1240	46.8	~ 1.5	5.29

inlet configuration and the background noise of the facility. In general it is found (CHC; Rose 1966, 1970; Mulhearn & Luxton 1975), that for values of τ less than four there is insufficient development time for $\overline{q^2}$ to grow. As seen in figures 7, 10 and 17(*b*), for larger τ both wind-tunnel and water-channel measurements exhibit turbulent growth between $\tau = 4$ and 5. Only when τ is calculated from the

measurements of KT taken behind grids separated from the inlet by relatively large values of τ is this behaviour not observed.

As seen in figure 17*b*) when the turbulent intensities of CHC and TC, after correcting for the virtual origin, are plotted *vs.* τ their evolutions appear to merge. The virtual origin was estimated from the intersection of the growing $u'/\bar{U}$ and $w'/\bar{U}$ data of TC (see figure 17*a*). It is reasonable to assume approximately the same virtual origin for the CHC measurements since the facility was the same and the inlets similar. TC's replacement of CHC's 0.318 cm square rods at the inlet with 0.508 cm round rods is almost accounted for (within 15%) by the associated decrease in drag coefficient.

As a last example consider the heat-flux measurements of Sreenivasan, Tavoularis & Corrsin (1982) obtained in a uniform mean shear to test gradient transport theory. STC reported that the turbulent transport $-\overline{\theta w}$ is, for some unknown reason, more efficient when $\partial\bar{U}/\partial z > 0$ than when $\partial\bar{U}/\partial z < 0$. In both cases, $\partial\bar{U}/\partial z$ had the same absolute magnitude and the temperature gradient induced negligible buoyancy effects on the flow. The effect of the sign of $\partial\bar{U}/\partial z$ on the temperature flux may be sought in the governing equations. The mean velocity gradient, however, appears neither in the temperature flux nor in the mean-square temperature-fluctuation equations. It appears only in the equation for the turbulent kinetic energy as $\overline{uw}(\partial\bar{U}/\partial z)$. However, since the net effect of $\overline{uw}(\partial\bar{U}/\partial z)$ is to decrease the mean kinetic energy of the flow, the sign of $\overline{uw}$ must compensate for the sign of $\partial\bar{U}/\partial z$ so that their product is always negative.

A possible explanation may be found if the relative values of τ for the two cases are compared. The measurements were taken at the same x-position and since the sign of τ is of no consequence, only the mean velocity and hence the convective time $x/\bar{U}$ may be different. From figure 2 of Sreenivasan *et al.* (1982), it is apparent that where the measurements were taken, the mean velocity for the $\partial\bar{U}/\partial z > 0$ data was less than the mean velocity for the $\partial\bar{U}/\partial z < 0$ data, and therefore τ was higher when $\partial\bar{U}\partial z > 0$. As suggested by the present results, the large values of τ are consistent with a higher value of $-\overline{\theta w}$ and hence a greater mixing rate.

9. Conclusions

The present study provides a clearer experimental understanding and simple global expression for the growth of turbulence in a uniform mean shear, for which there has previously been little agreement in the literature. The experiments reported here were conducted in a facility that is unique in that the effects of changing the magnitude of the mean shear on the turbulent growth could be isolated. Furthermore, for the first time, the influence of initial lengthscale disturbances on the far-downstream-growing turbulence was investigated. The turbulence intensity growth for the range of τ investigated (τ = 5–25) can be summarized by the following simple relations (16*a*, *b*):

$$\frac{u'}{\bar{U}} = C_1\left(\frac{x}{\bar{U}}\frac{\partial\bar{U}}{\partial z} - \frac{x_0}{\bar{U}}\frac{\partial\bar{U}}{\partial z}\right) = C_1(\tau - \tau_0),$$

$$\frac{w'}{\bar{U}} = C_2(\tau - \tau_0),$$

where x_0 is a function of the size of the initial disturbance and C_1 and C_2 are independent of x but may depend on the facility. Wind-tunnel measurements are

characterized equally well by (16) for τ in the same range as the present water-tunnel data.

If to a first approximation the characteristic time of the eddies (l/w') is proportional to the characteristic time of the mean flow $(\partial\bar{U}/\partial z)^{-1}$, as Tennekes & Lumley (1972) suggest, then (16) predicts that l must initially grow linearly with downstream distance, independent of the mean shear. Both wind-tunnel and water-channel measurements are in fairly good agreement with this prediction.

Equation (16) is an excellent approximation to the Tavoularis (1985) semi-analytical prediction for the growth of turbulence for moderate τ. This prediction was shown to be independent of his assumptions that $\overline{q^2}$ and $\overline{uw}(\partial\bar{U}/\partial z)$ are constant with z. Finally, this study raises the question of whether, even in an ideal uniform mean shear, some developing inhomogeneity along the mean shear should be expected.

The authors are indebted to Professor S. C. Corrsin for inspiration and fruitful discussions, and to Professor S. Tavoularis for additional help in interpreting earlier work. Funding for the present work was provided by the National Science Foundation under Grant OCE-8511289 and by the DARPA Fluid Dynamics URI program, Applied and Computational Mathematics Program, grant N00014-86-K-0758.

REFERENCES

BATCHELOR, G. K. & TOWNSEND, A. A. 1949 Decay of isotropic turbulence in the initial period. *Proc. R. Soc. Lond.* A **193**, 539.

CASTALDINI, M., HELLAND, K. N. & MALVESTUTO, V. 1980 Hot-film anemometry in aqueous NaCl solutions. *Intl J. Heat Mass Transfer* **24**, 133.

CHAMPAGNE, F. H., HARRIS, V. G. & CORRSIN, S. 1970 Experiments on nearly homogeneous turbulent shear flow. *J. Fluid Mech.* **41**, 81.

CORRSIN, S. 1963 Turbulence: experimental methods. In *Handbuch der Physik* VIII/2 (ed. S. Flugge & C. Truesdell), p. 524. Springer.

GRANT, H. L., STEWART, R. W. & MOILLIET, A. 1962 Turbulence spectra from a tidal channel. *J. Fluid Mech.* **12**, 241.

HARRIS, V. G., GRAHAM, A. A. & CORRSIN, S. 1977 Further experiments in nearly homogeneous turbulent shear flow. *J. Fluid Mech.* **81**, 657.

HASEN, E. M. 1967 Non-linear theory of turbulence onset in a shear flow. *J. Fluid Mech.* **29**, 721.

HELLAND, K. N., LII, K. S. & ROSENBLATT, M. 1977 Bispectra of atmospheric and wind tunnel turbulence. In *Proc. Symp. on Applications of Statistics* (ed. P. R. Krishnaiah), vol. 2, p. 123. Academic.

HINZE, J. O. 1975 *Turbulence*, 2nd edn. McGraw-Hill.

KÁRMÁN, T. VON 1937 The fundamentals of the statistical theory of turbulence. *J. Aero. Sci.* **4**, 131.

KARNIK, V. & TAVOULARIS, S. 1983 The asymptotic development of nearly homogeneous turbulent shear flow. *Turbulent Shear Flows* **4** (ed. L. J. S. Bradbury, F. Durst, B. E. Launder, F. W. Schmidt & J. H. Whitelaw), p. 14.18. Springer.

MULHEARN, P. J. & LUXTON, R. E. 1975 The development of turbulence structure in a uniform shear flow. *J. Fluid Mech.* **68**, 577.

OWEN, D. R. & ZIENKIEWICZ, H. K. 1957 The production of uniform mean shear flow in a wind tunnel. *J. Fluid Mech.* **2**, 521.

PHILLIPS, O. M. 1966 *Dynamics of the Upper Ocean.* Cambridge University Press.

PRANDTL, L 1925 *Z. angew. Math. Mech.* **5**, 136.

ROSE, W. G. 1966 Results of an attempt to generate a homogeneous turbulent shear flow. *J. Fluid Mech.* **25**, 97.

ROSE, W. G. 1970 Interaction of grid turbulence with a uniform mean shear. *J. Fluid Mech.* **44**, 767.

SREENIVASAN, K. R., TAVOULARIS, S. & CORRSIN, S. 1982 A test of gradient transport and its generalizations. *Turbulent Shear Flows* **3** (ed. L. J. S. Bradbury, F. Durst, B. E. Launder, F. W. Schmidt & J. H. Whitelaw), p. 96. Springer.

STILLINGER, D. C. 1983 The interpretation of statistics from hot-film anemometers used in salt water flows of variable temperature and density. *J. Phys.* E: *Sci. Instrum.* **15**, 1322.

STILLINGER, D. C., HEAD, M. J., HELLAND, K. N. & VAN ATTA, C. W. 1983 A closed loop gravity-driven water channel for density-stratified shear flows. *J. Fluid Mech.* **131**, 73.

TAVOULARIS, S. 1985 Asymptotic laws for transversely homogeneous turbulent shear flows. *Phys. Fluids* **28**, 999.

TAVOULARIS, S. & CORRSIN, S. 1981 Experiments in nearly homogeneous turbulent shear flows with a uniform mean temperature gradient, Part I. *J. Fluid Mech.* **104**, 311.

TENNEKES, H. & LUMLEY, J. L. 1972 *A First Course in Turbulence.* Massachusetts Institute of Technology Press.

WEBSTER, C. G. A. 1964 An experimental study of turbulence in a density stratified shear flow. *J. Fluid Mech.* **19**, 221.